

# FAST ALGORITHM FOR CONSTRAINED LINEAR INVERSE PROBLEMS

MOHAMMED RAYYAN SHERIFF, FLOOR FENNE REDEL, PEYMAN MOHAJERIN ESFAHANI

**ABSTRACT.** We consider the constrained Linear Inverse Problem (LIP), where a certain atomic norm (like the  $\ell_1$  and the Nuclear norm) is minimized subject to a quadratic constraint. Typically, such cost functions are non-differentiable which makes them not amenable to the fast optimization methods existing in practice. We propose two equivalent reformulations of the constrained LIP with improved convex regularity: (i) a smooth convex minimization problem, and (ii) a strongly convex min-max problem. These problems could be solved by applying existing acceleration based convex optimization methods which provide better  $O(1/k^2)$  theoretical convergence guarantee. However, to fully exploit the utility of these reformulations, we also provide a novel algorithm, to which we refer as the Fast Linear Inverse Problem Solver (FLIPS), that is tailored to solve the reformulation of the LIP. We demonstrate the performance of FLIPS on the sparse coding problem arising in image processing tasks. In this setting, we observe that FLIPS consistently outperforms the Chambolle-Pock and C-SALSA algorithms—two of the current best methods in the literature.

## 1. INTRODUCTION

Linear Inverse Problems simply refer to the task of recovering a signal from its noisy linear measurements. LIPs arise in many applications, such as image processing [14, 23, 2, 19], compressed sensing [11, 6, 7, 16], recommender systems [20], and control system engineering [18]. Formally, given a signal  $f \in \mathbb{H}$ , and its noisy linear measurements  $\mathbb{R}^n \ni x = \phi(f) + \xi$ , where,  $\phi : \mathbb{H} \rightarrow \mathbb{R}^n$  is a linear measurement operator and  $\xi \in \mathbb{R}^n$  is the measurement noise. The objective is to recover the signal  $f$  given its noisy measurements  $x$ , and the measurement operator  $\phi$ . Of specific interest is the case when the number of measurements available are fewer than the ambient dimension of the signal, i.e.,  $n < \dim(\mathbb{H})$ . In which case, we refer to the corresponding LIP as being ‘ill-posed’ since there could be potentially infinitely many solutions satisfying the measurements even for the noiseless case. In principle, one cannot recover a generic signal  $f$  from its measurements if the problem is ill-posed. However, the natural signals we encounter in practice often have much more structure to be exploited. For instance, natural images and audio signals tend to have a sparse representation in a well-chosen basis, matrix valued signals encountered in practice have low rank, etc. Enforcing such a low-dimensional structure into the recovery problem often suffices to overcome its ill-posedness. This is done by solving an optimization problem with an objective function that promotes the expected low-dimensional structure in the solution like sparsity, low-rank, etc. It is now well established that under very mild conditions, such optimization problems and even their convex relaxations often recover the true signal almost accurately [12, 11, 7].

---

*Date:* December 5, 2022.

The authors are with Delft Center for Systems and Control, Delft University of Technology, Delft, The Netherlands.

## 1.1. Problem setup

Given  $x \in \mathbb{R}^n$ , the linear operator  $\phi : \mathbb{H} \rightarrow \mathbb{R}^n$ , and  $\epsilon > 0$ , the object of interest in this article is the following optimization problem

$$\begin{cases} \operatorname{argmin}_{f \in \mathbb{H}} & c(f) \\ \text{subject to} & \|x - \phi(f)\| \leq \epsilon, \end{cases} \quad (1)$$

where  $\mathbb{H}$  is some finite-dimensional Hilbert space with the associated inner-product  $\langle \cdot, \cdot \rangle$ . The constraint  $\|x - \phi(f)\| \leq \epsilon$  is measured using the norm derived from an inner product on  $\mathbb{R}^n$  (it is independent from the inner product  $\langle \cdot, \cdot \rangle$  on the Hilbert space  $\mathbb{H}$ ).

The objective function is the mapping  $c : \mathbb{H} \rightarrow \mathbb{R}$  which is known to promote the low-dimensional characteristics desired in the solution. For example, if the task is to recover a sparse signal, we chose  $c(\cdot) = \|\cdot\|_1$ ; if  $\mathbb{H}$  is the space of matrices of a fixed order, then  $c(\cdot) = \|\cdot\|_*$  (the Nuclear-norm) if low-rank matrices are desired [8]. In general, the objective function is assumed to be *norm like*.

**Main challenges of (1) and existing state of the art methods to solve it.** One of the main challenges to tackle while solving (1) is that, the most common choices of the cost function  $c(\cdot)$  like the  $\ell_1$  norm, are not differentiable everywhere. In particular, the issue of non-differentiability gets amplified since it is prevalent precisely at the suspected optimal solution (sparse vectors). Thus, canonical gradient-based schemes do not apply to (1) with such cost functions. A common workaround is to use the notion of sub-gradients instead, along with a diminishing step-size. However, the Sub-Gradient Descent method (SGD) for generic convex problems converges only at a rate of  $O(1/\sqrt{k})$  [5]. For high-dimensional signals like images, this can be tiringly slow since the computational complexity scales exponentially with the signal dimensions.

## 1.2. Existing methods

The current best algorithms overcome the bottleneck of non differentiability in (1) by instead working with the more flexible notion of *proximal gradients*, and applying them to a suitable reformulation of the LIP (1). We primarily focus on two state-of-the-art methods in this article: the Chambolle-Pock algorithm (CP) [9] and the C-SALSA [1] algorithm, that solve the LIP (1).

(i) *The Chambolle-Pock algorithm:* Using the *convex indicator function*  $\mathbb{1}_{B[x,\epsilon]}(\cdot)$  of  $B[x,\epsilon]$ ,<sup>1</sup> the constraints in LIP (1) are incorporated into the objective function to get

$$\min_{f \in \mathbb{H}} c(f) + \mathbb{1}_{B[x,\epsilon]}(\phi(f)). \quad (2)$$

The indicator function  $\mathbb{1}_S(\cdot)$  of any closed convex set  $S$  is proper and lower-semicontinuous. Consequently, its convex-conjugate satisfies  $(\mathbb{1}_S^*)^* = \mathbb{1}_S$ . Since  $\mathbb{1}_{B[x,\epsilon]}^*(u) = \langle x, u \rangle + \epsilon\|u\|$ , for  $B[x,\epsilon]$  in particular, we have

$$\mathbb{1}_{B[x,\epsilon]}(\phi(f)) = \max_{u \in \mathbb{H}} \langle \phi(f), u \rangle - (\langle x, u \rangle + \epsilon\|u\|). \quad (3)$$

Incorporating (3) in (2), the LIP reduces to the following equivalent min-max formulation

$$\min_{f \in \mathbb{H}} \max_{u \in \mathbb{H}} c(f) + \langle \phi(f), u \rangle - (\langle x, u \rangle + \epsilon\|u\|). \quad (4)$$

The min-max problem (4) falls under a special subclass of convex-concave min-max problems with bi-linear coupling between the minimizing (f) and maximizing (u) variables. A primal-dual algorithm was proposed in [9, 10] to solve such problems under the condition that the mappings  $f \mapsto c(f)$  and  $u \mapsto \langle x, u \rangle + \epsilon\|u\|$  are proximal friendly. It turns out that in many relevant problems particularly where  $c(f) = \|f\|_1$  the proximal operator of  $f \mapsto c(f)$  is indeed easily computable [3]. Moreover, the proximal operator for the mapping

<sup>1</sup>The convex indicator function  $\mathbb{1}_S(z)$  of a given convex set  $S$  is  $\mathbb{1}_S(z) = 0$  if  $z \in S$ ;  $= +\infty$  if  $z \notin S$ .

$u \mapsto \langle x, u \rangle + \epsilon \|u\|$  corresponds to block soft-thresholding, and is also easy to implement. Under such a setting the CP algorithm has an ergodic convergence rate of  $O(1/k)$  for the duality gap of (4). This is already an improvement over the  $O(1/\sqrt{k})$  rate in canonical sub-gradient “descent” algorithms, and is currently the best convergence guarantee that exists for Problem (1).

(ii) *The C-SALSA algorithm:* The Constrained Split Augmented Lagrangian Shrinkage Algorithm (C-SALSA) [1] is an algorithm in which the Alternating Direction Method of Multipliers (ADMM) is applied to problem (2). For this problem, ADMM solves the LIP based on variable splitting using an Augmented Lagrangian Method (ALM). In a nutshell, the algorithm iterates between optimizing the variable  $f$  and the Lagrange multipliers until they converge. Even though the convergence rates for C-SALSA are not better than that of the CP algorithm, it is empirically found to be fast. Of particular interest is the case when  $\phi$  satisfies  $\phi^\top \phi = \mathbb{I}_n$ , in which case, further simplifications in the algorithm can be done that improve its speed for all practical purposes.

One of the objectives of this work is to provide an algorithm that is demonstrably faster than the existing methods, particularly for large scale problems. Given that solving an LIP is such a commonly arising problem in signal processing and machine learning, a fast and easy to implement is always desirable. This article precisely caters to this challenge. In [22], the LIP (1) was equivalently reformulated as a convex-concave min-max problem:

$$\min_{h \in B_c} \sup_{\lambda \in \Lambda} 2\sqrt{\langle \lambda, x \rangle - \epsilon \|\lambda\|} - \langle \lambda, \phi(h) \rangle, \quad (5)$$

where  $B_c = \{h \in \mathbb{H} : c(h) \leq 1\}$  and  $\Lambda := \{\lambda \in \mathbb{R}^n : \langle \lambda, x \rangle - \epsilon \|\lambda\| > 0\}$ . A solution to the LIP (1) can be computed from a saddle point  $(h^*, \lambda^*)$  of the min-max problem (5). Even though primal-dual schemes like Gradient Descent-Ascent with appropriate step-size can be used to compute a saddle-point of the min-max problem (5); such generic methods fail to exploit the specific structure of the min-max form (5). It turns out that equivalent problems with better convex regularity (like smoothness) can be derived from (5) by exploiting the specific nature of this min-max problem.

### 1.3. Contribution

In view of the existing methods mentioned above, we summarize the contributions of this work as follows:

- (a) **Exact reformulations with improved  $O(1/k^2)$  convergence rates.** We build upon the min-max reformulation (5) and proceed further on two fronts to obtain equivalent reformulations of the LIP (1) with better convex regularities. These reformulations open the possibility for applying acceleration based methods to solve the LIP (1) with faster rates of convergence  $O(1/k^2)$ , which improves upon the existing best rate of  $O(1/k)$ .
  - (i) *Exact smooth reformulation:* We explicitly solve the maximization over  $\lambda$  in (5) (Proposition 21) to obtain an equivalent smooth convex minimization problem (Theorem 5).
  - (i) *Strongly convex min-max reformulation:* We propose a new min-max reformulation (21) that is slightly different from (5) and show that it has strong-concavity in  $\lambda$  (Lemma 13). This allows us to apply accelerated version of the Chambolle-Pock algorithm [10, Algorithm 4]; which converges at a rate of  $O(1/k^2)$  in duality gap for ergodic iterates (Remark 14)
- (b) **Tailored fast algorithm:** We present a novel algorithm (Algorithm 1) called the Fast LIP Solver (FLIPS), which exploits the structure of the proposed smooth reformulation (14) better than the standard acceleration based methods. The novelty of FLIPS is that it combines ideas from canonical gradient descent schemes to find a descent direction; and then from the Frank-Wolfe (FW) algorithm [17] in taking a step in the descent direction. We provide an explicit characterization of the optimal step size which could be computed without significant additional computations. We show empirically on

standard image processing tasks like denoising, that the proposed algorithm outperforms the state-of-the-art convex programming based methods for (1) like CP and C-SALSA in most metrics of convergence speed.

- (c) **Open source Matlab package:** Associated with this algorithm, we also present an open-source Matlab package that includes the proposed algorithm (and also the implementation of CP and C-SALSA) [21].

This article is organized as follows. In Section 2 we discuss two equivalent reformulations of the LIP; one as a smooth minimization problem in subsection 2.1, and then as a min-max problem with strong-convexity in subsection 2.2. Subsequently, in Section 3 the FLIPS algorithm is presented, followed by the numerical simulations in section 4. All the proofs of results in this article are relegated towards the end of this article in Section 5 for better readability.

**Notations.** Standard notations have been employed for the most part. The interior of a set  $\mathcal{S}$  as  $\text{int}(\mathcal{S})$ . The  $n \times n$  identity matrix is denoted by  $\mathbb{I}_n$ . For a matrix  $M$  we let  $\text{tr}(M)$  and  $\text{image}(M)$  denote its trace and image respectively. The gradient of a continuously differentiable function  $\eta(\cdot)$  evaluated at a point  $h$  is denoted by  $\nabla\eta(h)$ .

Generally  $\|\cdot\|$  is the norm associated with the inner product  $\langle \cdot, \cdot \rangle$  of the Hilbert space  $\mathbb{H}$ , unless specified otherwise explicitly. Given two Hilbert spaces  $(\mathbb{H}_1, \langle \cdot, \cdot \rangle_1)$  and  $(\mathbb{H}_2, \langle \cdot, \cdot \rangle_2)$  and a linear map  $T : \mathbb{H}_1 \rightarrow \mathbb{H}_2$ , its adjoint  $T^a$  is another linear map  $T^a : \mathbb{H}_2 \rightarrow \mathbb{H}_1$  such that  $\langle v, T(u) \rangle_2 = \langle T^a(v), u \rangle_1$  for all  $u \in \mathbb{H}_1$  and  $v \in \mathbb{H}_2$ .

## 2. EQUIVALENT REFORMULATIONS WITH IMPROVED CONVEX REGULARITY

We consider the LIP (1) under the setting of following two assumptions that are enforced throughout the article.

**Assumption 1** (Cost function). *The cost function  $c : \mathbb{H} \rightarrow \mathbb{R}$  is*

- (a) positively homogenous: *For every  $r \geq 0$  and  $f \in \mathbb{H}$ ,  $c(rf) = rc(f)$*
- (b) inf compact: *the unit sub-level set  $B_c := \{f \in \mathbb{H} : c(f) \leq 1\}$  is compact*
- (c) quasi convex: *the unit sub-level set  $B_c$  is convex.*

In addition to the conditions in Assumption 1, if the cost function is symmetric about the origin, i.e.,  $c(-f) = c(f)$  for all  $f \in \mathbb{H}$ , then it is indeed a *norm* on  $\mathbb{H}$ . Thus, many common choices like the  $\ell_1$  and Nuclear norms for practically relevant LIPs are included in the setting of Assumption 1.

**Assumption 2** (Strict feasibility). *We shall assume throughout this article that  $\|x\| > \epsilon > 0$  and that the corresponding LIP (1) is strictly feasible, i.e., there exists  $f \in \mathbb{H}$  such that  $\|x - \phi(f)\| < \epsilon$ .*

### 2.1. Reformulation as a *smooth* minimization problem

Let the mapping  $e : \mathbb{R}^n \rightarrow [0, +\infty)$  be defined as

$$e(h) := \min_{\theta \in \mathbb{R}} \|x - \theta\phi(h)\|^2 = \begin{cases} \|x\|^2 & \text{if } \phi(h) = 0, \\ \|x\|^2 - \frac{|\langle x, \phi(h) \rangle|^2}{\|\phi(h)\|^2} & \text{otherwise.} \end{cases} \quad (6)$$

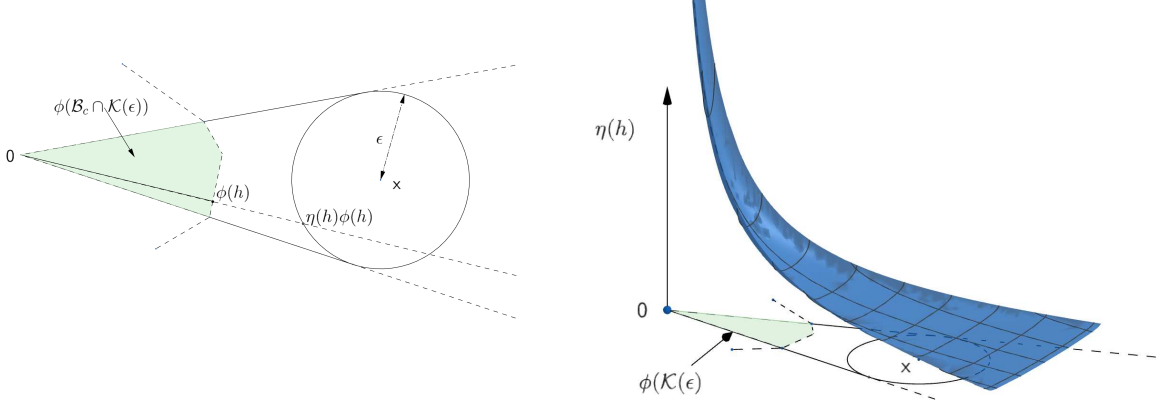
Consider the family of convex cones  $\{\mathcal{K}(\bar{\epsilon}) : \bar{\epsilon} \in (0, \epsilon]\}$  defined by

$$\mathcal{K}(\bar{\epsilon}) := \{h \in \mathbb{H} : \langle x, \phi(h) \rangle > 0, \text{ and } e(h) \leq \bar{\epsilon}^2\}, \text{ for every } \bar{\epsilon} \in (0, \epsilon]. \quad (7)$$

Equivalently, observe that  $h \in \mathcal{K}(\bar{\epsilon})$  if and only if  $\langle x, \phi(h) \rangle \geq \|\phi(h)\| \sqrt{(\|x\|^2 - \bar{\epsilon}^2)}$ . Therefore, it is immediately evident that  $\mathcal{K}(\bar{\epsilon})$  is convex for every  $\bar{\epsilon} \in (0, \epsilon]$ .

**Definition 1** (New objective function). Consider  $x, \phi$ , and  $\epsilon > 0$  such that Assumption 2 holds, and let the map  $\eta : \mathcal{K}(\epsilon) \rightarrow [0, +\infty)$  be defined by

$$\eta(h) := \frac{\|x\|^2 - \epsilon^2}{\langle x, \phi(h) \rangle + \|\phi(h)\| \sqrt{\epsilon^2 - e(h)}}. \quad (8)$$



(A) Diagram presenting the relation between  $\phi(B_c \cap \mathcal{K}(\epsilon))$ ,  $h$ ,  $\eta(h)$ ,  $\phi(h)$ ,  $x$  and  $\epsilon$ .

(B) Diagram presenting the  $\eta(h)$  evaluated over  $\phi(\mathcal{K}(\epsilon))$ .

FIGURE 1. Graphical overview of  $\eta, \phi(\mathcal{K}(\epsilon))$ .

**Remark 2** (Physical interpretation of  $\eta(h)$ ). For any  $h \in \mathcal{K}(\epsilon)$ , the value  $\eta(h)$  is the minimum amount by which the point  $\phi(h) \in \mathbb{R}^n$  must be scaled positively so that it is contained in the closed neighbourhood  $B[x, \epsilon]$  of  $x$  as depicted in Figure 1a.

**Proposition 3** (Derivatives of  $\eta$ ). Consider  $x, \phi, \epsilon > 0$  such that Assumption 2 holds, and  $\eta(h)$  as defined in (8). then the following assertions hold.

(i) **Convexity:** The function  $\eta : \mathcal{K}(\epsilon) \rightarrow [0, +\infty)$  is convex.

(ii) **Gradients:** The function  $\eta : \mathcal{K}(\epsilon) \rightarrow [0, +\infty)$  is differentiable at every  $h \in \text{int}(\mathcal{K}(\epsilon)) = \{h \in \mathbb{H} : \langle x, \phi(h) \rangle > 0, \text{ and } e(h) < \epsilon^2\}$ , and the derivative is given by

$$\nabla \eta(h) = \frac{-\eta(h)}{\|\phi(h)\| \sqrt{\epsilon^2 - e(h)}} \phi^a(x - \eta(h) \phi(h)) \quad \text{for all } h \in \text{int}(\mathcal{K}(\epsilon)), \quad (9)$$

where  $\phi^a$  is the adjoint operator of  $\phi$ .

(iii) **Hessian:** the function  $\eta : \mathcal{K}(\epsilon) \rightarrow [0, +\infty)$  is twice continuously differentiable at every  $h \in \text{int}(\mathcal{K}(\epsilon))$ . The hessian is the linear operator

$$\mathbb{H} \ni v \mapsto (\Delta^2 \eta(h))(v) := (\phi^a \circ M(h) \circ \phi)(v) \in \mathbb{H}, \quad (10)$$

where  $M : \text{int}(\mathcal{K}(\epsilon)) \rightarrow \mathbb{R}^n \times \mathbb{R}^n$  is a continuous matrix-valued map.<sup>2</sup>

**Challenges for smoothness:** As such, the mapping  $\eta : B_c \cap \mathcal{K}(\epsilon) \rightarrow \mathbb{R}$  is not smooth, and the issue arises due to two reasons. (i) First of all, consider any  $h \in B_c \cap \mathcal{K}(\epsilon)$ , then it is immediate from (8) that  $\eta(\theta h) = \frac{C}{\theta}$  for some  $C > 0$ . Thus,  $\eta$  achieves arbitrarily large values (and arbitrarily high curvature) as  $\|h\| \rightarrow 0$  as shown in Figure 1b as a simple example. Thereby, the mapping  $(0, 1] \ni \theta \mapsto \eta(\theta h)$  is not smooth, and consequently, the mapping  $\eta : B_c \cap \mathcal{K}(\epsilon) \rightarrow \mathbb{R}$  cannot be smooth. (ii) Secondly, it must be observed that  $\eta$  is not differentiable on the boundary of the cone  $\mathcal{K}(\epsilon)$ . Moreover, as  $e(h) \uparrow \epsilon^2$ , i.e.,  $h$  approaches the boundary

<sup>2</sup>Please see (43) for the precise definition of  $M(h)$ .

of the cone  $\mathcal{K}(\epsilon)$  from its interior, it is apparent from (9) that the gradients of  $\eta$  are unbounded. It turns out that by avoiding these two scenarios (which will be made more formal shortly),  $\eta$  is indeed smooth.

**Proposition 4** (Convex regularity of  $\eta$ ). *Consider the LIP in (1) under the setting of Assumption 2 with  $c^*$  being its optimal value. For every  $\hat{\eta} > c^*$  and  $\bar{\epsilon} \in (0, \epsilon)$ , consider the convex set*

$$\mathcal{H}(\bar{\epsilon}, \hat{\eta}) := \{h \in B_c \cap \mathcal{K}(\bar{\epsilon}) : \eta(h) \leq \hat{\eta}\}. \quad (11)$$

- (i) **Smoothness:** *There exist constant  $\beta \in (0, +\infty)$ , such that the mapping  $\eta : \mathcal{H}(\bar{\epsilon}, \hat{\eta}) \rightarrow [0, +\infty)$  is  $\beta$ -smooth. In other words, the inequality*

$$\|\nabla\eta(h) - \nabla\eta(h')\| \leq \beta \|h - h'\| \text{ holds for all } h, h' \in \mathcal{H}(\bar{\epsilon}, \hat{\eta}). \quad (12)$$

- (ii) **Strong convexity:** *In addition, if the linear operator  $\phi$  is invertible, then there exists constant  $\alpha > 0$ , such that the mapping  $\eta : \mathcal{H}(\bar{\epsilon}, \hat{\eta}) \rightarrow [0, +\infty)$  is  $\alpha$ -strongly convex. In other words, the inequality*

$$\eta(h') \geq \eta(h) + \langle \nabla\eta(h), h' - h \rangle + \frac{1}{2}\alpha \|h' - h\|^2 \text{ holds for all } h, h' \in \mathcal{H}(\bar{\epsilon}, \hat{\eta}). \quad (13)$$

The precise value of regularity parameters  $\alpha$  and  $\beta$  are provided in Remarks 9 and 10 respectively.

**Theorem 5** (Smooth reformulation). *Consider the LIP (1) under the setting of Assumption 1 and 2, and let  $c^*$  be its optimal value. Then the following assertions hold*

- (i) *Every optimal solution  $f^*$  of the LIP (1) satisfies  $e(f^*) < \epsilon^2$ .*  
(ii) **The smooth problem:** *Consider any  $(\bar{\epsilon}, \hat{\eta})$  such that  $e(f^*) \leq \bar{\epsilon}^2 < \epsilon^2$  and  $c^* < \hat{\eta}$ . Then the optimization problem*

$$\min_{h \in \mathcal{H}(\bar{\epsilon}, \hat{\eta})} \eta(h). \quad (14)$$

*is a smooth convex optimization problem equivalent to the LIP (1). In other words, the optimal value of (14) is equal to  $c^*$  and  $h^*$  is a solution to (14) if and only if  $c^*h^*$  is an optimal solution to (1).*

**Remark 6** (Choosing  $\bar{\epsilon}$ ). Consider the problem of recovering some true signal  $f^*$  from its noisy linear measurements  $x = \phi(f^*) + \xi$ , where  $\xi$  is some additive measurement noise. Then,  $\epsilon$  is chosen in (1) such that the probability  $\mathbb{P}(\|\xi\| \leq \epsilon)$  is very high. Then for any  $\bar{\epsilon} \in (0, \epsilon)$  we have  $e(f^*) < \bar{\epsilon}^2$  with probability at least  $\mathbb{P}(\|\xi\| \leq \epsilon) \cdot \mathbb{P}\left(\left|\left\langle \xi, \frac{\phi(f^*)}{\|\phi(f^*)\|} \right\rangle\right|^2 > \epsilon^2 - \bar{\epsilon}^2\right)$ . Thus, in practise, one could select  $\bar{\epsilon}$  to be just smaller than  $\epsilon$  based on available noise statistics. For empirical evidence, we have demonstrated in Section 4.2 by plotting the histogram of  $e(f^*)$  for 28561 instances of LIPs arising in a single image denoising problem solved with a fixed value of  $\epsilon$ . It is evident from Figure (8) that there is a strict separation between the value  $\epsilon^2$ , and the maximum value of  $e(f^*)$  among different LIPs.

**Remark 7** (Choosing the upper bound  $\hat{\eta}$ ). Since  $\hat{\eta}$  is any upper bound to the optimal value  $c^*$  of the LIP (1), and equivalently (14), a simple candidate is to use  $\hat{\eta} = \eta(h)$  for any feasible  $h$ . In particular, for  $h_0 = (1/c(f'))f'$ , where  $f' := \arg\min_f \|x - \phi(f)\|^2$  is the solution to the least squares problem, it can be shown that

$$\hat{\eta} := \eta(h_0) = c(f') \left(1 - \sqrt{1 - \frac{\|x\|^2 - \epsilon^2}{\|x'\|^2}}\right) \text{ where } x' = \phi(f'). \quad (15)$$

We would like to emphasise that the value of  $\hat{\eta}$  is required only to conclude smoothness of (14) and the corresponding smoothness constants. It is *not necessary* for the implementation of the proposed algorithm FLIPS. The inequality  $\eta(h) \leq \hat{\eta}$  in the constraint  $h \in \mathcal{H}(\bar{\epsilon}, \hat{\eta})$  is ensured for all iterates of FLIPS as it generates a sequence of iterates such that  $\eta$  is monotonically decreasing.

**Remark 8** (Choosing the lower bound  $\bar{\eta}$ ). Let  $c'(f) := \max_{h \in B_c} \langle f, h \rangle$  denote the dual function of  $c$ . Then the quantity

$$\bar{\eta} = \frac{\|x\| (\|x\| - \epsilon)}{c'(\phi^a(x))}, \quad (16)$$

is a positive lower bound to the optimal value  $c^*$  of the LIP (1).<sup>3</sup>

**Remark 9** (Strong convexity parameter). Let  $\bar{\sigma}(\phi^a \circ \phi)$  be the minimum eigenvalue of the linear operator  $(\phi^a \circ \phi)$ , then for any  $\bar{\eta} \in (0, c^*]$ , the constant

$$\alpha(\bar{\eta}) = \frac{2\bar{\eta}^3}{(\|x\|^2 - \epsilon^2)} \bar{\sigma}(\phi^a \circ \phi), \quad (17)$$

satisfies the strong-convexity condition (13).

**Remark 10** (Smoothness parameter). Let  $\hat{\sigma}(\phi^a \circ \phi)$  be the maximum eigenvalue of the linear operator  $(\phi^a \circ \phi)$ , then for any  $\hat{\eta} \geq c^*$ , and  $\bar{\epsilon} > 0$  such that  $e(f^*) \leq \bar{\epsilon}^2 < \epsilon^2$ , the constant

$$\beta(\bar{\epsilon}, \hat{\eta}) = \frac{\epsilon^2 \hat{\eta}^3}{(\epsilon^2 - \bar{\epsilon}^2)^{3/2}} \frac{(\|x\| + \epsilon)}{(\|x\| - \epsilon)^2} \hat{\sigma}(\phi^a \circ \phi), \quad (18)$$

satisfies the smoothness condition (12).

**Remark 11** (Applying accelerated gradient descent for (14)). Reformulating the LIP (1) as the smooth minimization problem (14) allows us to apply accelerated gradient descent methods [25, 3], to improve the theoretical convergence rate from  $O(1/k)$  to  $O(1/k^2)$ . We know that by applying the projected accelerated gradient descent algorithm [3] for (14)

$$\begin{cases} z_k = \Pi_{\mathcal{H}(\bar{\epsilon}, \hat{\eta})} \left( h_k - (1/b) \nabla \eta(h_k) \right) \\ t_{k+1} = \frac{1 + \sqrt{1 + 4t_k^2}}{2} \\ h_{k+1} = z_k + \frac{t_k - 1}{t_{k=1}} (z_k - z_{k-1}), \end{cases} \quad (19)$$

the sub-optimality  $\eta(h_k) - c^*$  diminishes at a rate of  $O(1/k^2)$ , which is an improvement over the existing best rate of  $O(1/k)$  for the CP algorithm. Moreover, if the linear map  $\phi$  is invertible, then since the objective function  $\eta(c)$  is strongly convex, the iterates in (19) (or even simple projected gradient descent) converge exponentially (with a slightly different step-size rule).

One of the challenges in implementing the algorithm (19) is that it might not be possible in general, to compute the orthogonal projections onto the set  $\mathcal{H}(\bar{\epsilon}, \hat{\eta})$ . However, if somehow the inequality  $e(h_k) \leq \bar{\epsilon}^2$  is ensured always along the iterates, then the problem of projection onto the set  $\mathcal{H}(\bar{\epsilon}, \hat{\eta})$  simply reduces to projecting onto the set  $B_c$ , which is relatively much easier. In practice, this can be achieved by selecting  $\bar{\epsilon}$  such that  $e(f^*) < \bar{\epsilon}^2 < \epsilon^2$ , and a very small step-size  $(1/b)$  so that the iterates  $(h_k)_k$  do not violate the inequality  $e(h_k) < \bar{\epsilon}^2$ . This is precisely how the algorithm (19) is implemented in the image denoising problem of Figure 8. In fact, we have observed empirically that one can tune the value of  $b$  for a given LIP so that the criterion:  $e(h_k) < \bar{\epsilon}^2$  is always satisfied. However, if one has to solve a number of LIPs for various values of  $x$  via algorithm (19); tuning the value(s) of  $b$  could be challenging and tedious. Thus, applying off-the shelf accelerated methods directly to the smooth reformulation (14) might not be the best choice. This is one of the reasons we propose a different algorithm (FLIPS) that is tailored to solve the smooth reformulation.

<sup>3</sup>Since  $rx \in \Lambda$  for all  $r > 0$ , interchanging the order of min-max in (5), we see that

$$c^* = \max_{\lambda \in \Lambda} \left\{ 2\sqrt{\langle \lambda, x \rangle - \epsilon \|\lambda\|} - c'(\phi^a(\lambda)) \right\} \geq \max_{r>0} \left\{ 2\sqrt{r} \sqrt{\|x\|^2 - \epsilon \|x\|} - rc'(\phi^a(x)) \right\} = \bar{\eta}.$$



## 2.2. Equivalent min-max problem with strong-convexity

**Lemma 12** (Min-max reformulation with strong convexity). *Consider the LIP (1) under the setting of Assumptions 1 and 2, and let  $c^*$  denote its optimal value. For every  $\bar{\eta}, \hat{\eta}, \bar{\epsilon} > 0$  such that  $\bar{\eta} \leq c^* < \hat{\eta}$  and  $e(f^*) \leq \bar{\epsilon}^2 < \epsilon^2$ , let  $B > 0$  be a constant and the set  $\Lambda(\bar{\eta}, B) \subset \mathbb{R}^n$  be defined by*

$$\begin{cases} B := \frac{\epsilon \hat{\eta}^2}{(\|x\|^2 - \epsilon^2)\sqrt{\epsilon^2 - \bar{\epsilon}^2}} \\ \Lambda(\bar{\eta}, B) := \{\lambda \in \Lambda : l(\lambda) \geq \bar{\eta} \text{ and } \|\lambda\| \leq B\}. \end{cases} \quad (20)$$

Then the min-max problem

$$\begin{cases} \min_{h \in B_c} \sup_{\lambda \in \Lambda(\bar{\eta}, B)} L(\lambda, h) = 2l(\lambda) - \langle \lambda, \phi(h) \rangle, \end{cases} \quad (21)$$

is equivalent to the LIP (1). In other words, a pair  $(h^*, \lambda^*) \in B_c \times \Lambda(\bar{\eta}, B)$  is a saddle point of (21) if and only if  $c^*h^*$  is an optimal solution to the LIP (1), and  $\lambda^* = \lambda(h^*)$ .

The min-max problem (12) falls into the interesting class of convex-concave min-max problems with a bi-linear coupling between the minimizing variable  $h$  and the maximizing variable  $\lambda$ . Incorporating the constraints  $h \in B_c$  and  $\lambda \in \Lambda(\bar{\eta}, B)$  with indicator functions, the min-max problem writes

$$\begin{cases} \min_{h \in \mathbb{H}} \max_{\lambda \in \mathbb{R}^n} \mathbf{1}_{B_c}(h) - \langle \lambda, \phi(h) \rangle - (\mathbf{1}_{\Lambda(\bar{\eta}, B)}(\lambda) - 2l(\lambda)). \end{cases}$$

If the constraint sets  $B_c$  and  $\Lambda(\bar{\eta}, B)$  are projection friendly, the min-max problem (12) can be solved by directly applying the Chambolle-Pock (CP) primal-dual algorithm. Without any further assumptions, the duality gap of min-max problem (21) converges at a rate of  $O(1/k)$  for the Chambolle-Pock algorithm. This rate of convergence is currently the best, and same as the one when CP is applied directly to the min-max problem (4) discussed in the introduction. However, in addition, if the mapping  $\Lambda(\bar{\eta}, B) \ni \lambda \mapsto -2l(\lambda)$  is smooth and strongly convex, acceleration techniques can be incorporated into the Chambolle-Pock algorithm. One of the contribution of this article towards this direction is to precisely establish that indeed this mapping is smooth and strongly concave under the setting of Assumption 2. in which case, the rate of convergence improves from  $O(1/k)$  to  $O(1/k^2)$ .

**Lemma 13** (Convex regularity in min-max reformulation). *Consider  $x \in \mathbb{R}^n$  and  $\epsilon > 0$  such that  $\|x\| > \epsilon$ . For any  $\bar{\eta}, \hat{\eta}, \bar{\epsilon} > 0$  such that  $\bar{\eta} \leq c^* < \hat{\eta}$  and  $e(f^*) \leq \bar{\epsilon}^2 < \epsilon^2$ ; let  $B > 0$  be as given in (20), and let  $\alpha', \beta'$  be constants given by*

$$\alpha' := \frac{\epsilon}{(\|x\|^2 - \epsilon^2)} \left(\frac{\bar{\eta}}{B}\right)^3 \quad \text{and} \quad \beta' := \frac{(\|x\|^2 - \epsilon^2)}{2\bar{\eta}^3}. \quad (22)$$

Then the mapping  $\Lambda(\bar{\eta}, B) \ni \lambda \mapsto -2l(\lambda)$  is  $\alpha'$ -strongly convex and  $\beta'$ -smooth.

**The Accelerated Chambolle-Pock algorithm.** In view of the Lemmas 12 and 13, the min-max problem (21) admits an accelerated version of the Chambolle-Pock algorithm [10, Algorithm 4, (30)]. Denoting  $\Pi_{B_c}$  and  $\Pi_{\Lambda(\bar{\eta}, B)}$  to be the projection operators onto the sets  $B_c$  and  $\Lambda(\bar{\eta}, B)$  respectively, and  $(\alpha', \beta') = (\alpha'(\bar{\eta}, B), \beta'(\bar{\eta}))$  for simplicity, the accelerated CP algorithm for (21) is

$$\begin{cases} h_{k+1} = \Pi_{B_c} \left( h_k + s_k \phi^a(\lambda_k + \theta_k(\lambda_k - \lambda_{n-1})) \right) \\ \lambda_{k+1} = \Pi_{\Lambda(\bar{\eta}, B)} \left( \lambda_k + \frac{t_k}{l(\lambda_k)} \left( x - (\epsilon/\|\lambda_k\|)\lambda_k + l(\lambda_k)\phi(h_{k+1}) \right) \right), \end{cases} \quad (23)$$

where,  $(t_k, s_k, \theta_k)$  are positive real numbers satisfying

$$\theta_{k+1} = \frac{1}{\sqrt{1 + \alpha' t_k}}, \quad t_{k+1} = \frac{t_k}{\sqrt{1 + \alpha' t_k}}, \quad \text{and} \quad s_{k+1} = s_k \sqrt{1 + \alpha' t_k}, \quad \text{for } n \geq 0, \quad (24)$$



with  $\theta_0 = 1$ ,  $t_0 = \frac{1}{2\beta'}$ , and  $s_0 = \frac{\beta'}{\|\phi\|_o^2}$ .

**Remark 14** (Ergodic  $O(1/k^2)$  rate of convergence). Consider the min-max problem (21), and let  $(h_k, \lambda_k)$  for  $n = 1, 2, \dots$ , be the sequence generated by the Accelerated CP algorithm (23). Then there exists a constant  $C > 0$  such that

$$\max_{\lambda \in \Lambda(\bar{\eta}, B)} L(h_k, \lambda) - \min_{h \in B_c} L(h, \lambda_k) \leq \frac{C}{k^2} \quad \text{for all } n \geq 1.$$

The remark is an immediate consequence of Lemma 13 and [10, Theorem 4 and Lemma 2].

**Remark 15** (Projection onto the set  $\Lambda(\bar{\eta}, B)$ ). In general, computing projections onto the set  $\Lambda(\bar{\eta}, B)$  is non-trivial, and in principle, requires a sub problem to be solved at each iteration. However, since the duality gap along the iterates  $(h_k, \lambda_k)$  generated by (23) converges to zero; it follows that  $c^* = \lim_{k \rightarrow +\infty} l(\lambda_k)$ . By selecting  $\bar{\eta} < c^*$ , computing projections onto the set  $\Lambda(\bar{\eta}, B)$  becomes trivial for all but finitely many iterates in the sequence  $(\lambda_k)_k$ . To see this, observe that the set  $\Lambda(\bar{\eta}, B)$  is the intersection of two convex sets  $\{\lambda : \|\lambda\| \leq B\}$  and  $\{\lambda : l(\lambda) \geq \bar{\eta}\}$ . Since  $c^* = \lim_{k \rightarrow +\infty} l(\lambda_k)$ , the inequality  $l(\lambda_k) \geq \bar{\eta}$  is readily satisfied for all but finitely many iterates if  $\bar{\eta} < c^*$ . Consequently, all but finitely many iterates in the sequence  $(\lambda_k)_k$  are contained in the set  $\{\lambda : l(\lambda) \geq \bar{\eta}\}$ . Therefore, computing projections onto the set  $\Lambda(\bar{\eta}, B)$  eventually reduces to projecting onto the set  $\{\lambda : \|\lambda\| \leq B\}$ , which is trivial.

### 3. THE FAST LIP SOLVER

Even though the newly proposed smooth reformulation of (1) is amenable to acceleration based schemes; it could suffer in practice from conservative estimation of smoothness constant. Moreover, since one has to ensure that  $h \in \mathcal{K}(\epsilon)$  for all the iterates, it further constrains the maximum step-size that could be taken, which results in slower convergence in practice. These issues make applying off-the shelf methods to solve the proposed smooth problem not fully appealing. To overcome this, we propose the Fast LIP Solver (FLIPS), presented in Algorithm 1.

---

#### Algorithm 1: The Fast LIP Solver

---

**Input:** Measurement  $x$ , linear operator  $\phi$ ,  $\epsilon > 0$ , and oracle parameters.

**Output:** Sparse representation  $f^*$

*Initialise:*  $h_0 = (1/c(f'))f'$ , where  $f' = \phi \setminus x := \operatorname{argmin}_f \|x - \phi(f)\|$ .

*Check for strict feasibility (Assumption 2)*

*Iterate till convergence*

- 1 **Compute the update direction  $g(h)$  using any viable oracle**
- 2 **Exact line search:** Compute

$$\gamma(h) = \begin{cases} \operatorname{argmin}_{\gamma \in [0,1]} & \eta(h + \gamma(g(h) - h)) \\ \text{subject to} & h + \gamma(g(h) - h) \in \mathcal{K}(\bar{\epsilon}) \end{cases}$$

- 3 *Update* :  $h^+ = h + \gamma(h)(g(h) - h)$

- 4 **Check for stopping criteria**

*Repeat*

- 5 **Output:** the sparse representation  $f^* = \eta(h)h$ .
- 

In a nutshell, FLIPS uses two oracle calls in each iteration; one each to compute an update direction  $g(h)$  and the step-size  $\gamma(h)$ . It then updates the current iterate by taking the convex combination  $h^+ = h + \gamma(h)(g(h) - h)$  controlled by  $\gamma(h)$ . This is repeated until a convergence criterion is met.

**Remark 16** (Initialization and checking feasibility). The algorithm is initialised with a normalized solution of the least squares problem:  $\operatorname{argmin}_f \|x - \phi(f)\|$ , which is written as  $\phi \setminus x$  following the convention used in Matlab. If the LIP is ill-posed, the least squares problem will have infinitely many solutions. Even though the algorithm works with any initialization among the solutions to the least squares problem, it is recommended to use the minimum  $\ell_2$ -norm solution  $f' = \phi^\dagger x$ . Since  $\phi(f')$  is closest point (w.r.t. the  $\|\cdot\|$  used in the least squares problem), it is easily verified that the LIP satisfies the strict feasibility condition in Assumption 2 if and only if the inequality  $\|x - \phi(f')\| < \epsilon$  holds.

**Remark 17** (Constraint splitting and successive feasibility). The novelty of FLIPS is that it combines ideas from canonical gradient descent methods to compute the update direction, but takes a step in spirit similar to that of the Frank-Wolfe algorithm. This allows us to perform a sort of constraint splitting and handle different constraints in (14) separately. To elaborate, recall that the feasible set in (14) is

$$\mathcal{H}(\bar{\epsilon}, \hat{\eta}) = \{h \in B_c \cap \mathcal{K}(\bar{\epsilon}) : \eta(h) \leq \hat{\eta}\}.$$

On the one hand, since  $B_c$  is a convex set, for a given  $h \in B_c$ , the direction oracle guarantees that  $h^+ \in B_c$  by producing  $g(h) \in B_c$  at every iteration. On the other hand, selection of  $\gamma(h)$  in the exact line search oracle ensures that  $\eta(h^+) \leq \eta(h) \leq \hat{\eta}$  and  $h^+ \in \mathcal{K}(\bar{\epsilon})$ . Thus,  $h^+ \in \mathcal{H}(\bar{\epsilon}, \hat{\eta})$ , and

### 3.1. Descent direction oracle

For any given  $h \in \mathcal{H}(\bar{\epsilon}, \hat{\eta})$  (in principle, for any  $h \in \mathcal{K}(\bar{\epsilon})$ ), the task of the direction oracle is to simply produce a direction  $g(h) \in B_c$  along which the function  $\eta(\cdot)$  could be minimized. This is usually done by solving a sub-problem at every iteration, and thus, depending on the complexity of these sub-problems, different direction oracle could be had.

- (a) **Linear Oracle:** As the name suggests, the direction  $g(h)$  is found by solving a linear optimization problem over  $B_c$

$$g(h) \in \left\{ \operatorname{argmin}_{g \in B_c} \langle \nabla \eta(h), g \rangle. \right. \quad (25)$$

Finding the update direction  $d(h)$  via a linear oracle, makes the corresponding implementation of FLIPS very similar to the Frank-Wolfe algorithm [15, 17], but with constraint splitting as discussed earlier. The only difference is that the linear sub-problem (25) is not solved over the entire feasible set  $\mathcal{H}(\bar{\epsilon}, \hat{\eta})$ , but instead, it is solved only over the set  $B_c$ .

**Example 1** (Linear oracle for sparse coding). For the sparse coding problem, i.e., LIP (1) with  $c(f) = \|f\|_1$ , the corresponding linear oracle (25) is easily described due to the Hölder inequality [24]. The  $i$ -th component  $g_i(h)$  of the direction  $g(h)$  is given by

$$g_i(h) = \begin{cases} -\operatorname{sgn}(\partial \eta / \partial h_i), & \text{if } |\partial \eta / \partial h_i| = \|\nabla \eta(h)\|_\infty, \\ 0, & \text{if } |\partial \eta / \partial h_i| \neq \|\nabla \eta(h)\|_\infty. \end{cases} \quad (26)$$

- (b) **Quadratic Oracle:** As indicative of the name, the update direction  $g(h)$  is computed for any given  $h$  by solving a quadratic problem. The complexity of implementing a quadratic oracle is more than that of the linear oracle as it solves a quadratic problem over the linear one. Solving this quadratic problem essentially reduces to computing orthogonal projections of points onto the set  $B_c$ , which we denote by the operator  $\Pi_{B_c}(\cdot)$ . Thus, a practical assumption in implementing a quadratic oracle is that the set  $B_c$  is projection friendly. For some LIPs like the matrix completion problem, solving the corresponding projection problem requires computing the SVD at every iteration, which could be challenging for large scale problems. However, for other relevant problems like BPDN, the corresponding projection problem requires projection onto the  $\ell_1$ -sphere which is easy to implement [13].

(i) *Simple quadratic oracle*: For any given  $h$ , this oracle solves the quadratic problem

$$g(h) = \left\{ \operatorname{argmin}_{g \in B_c} \langle \nabla \eta(h), g \rangle + (\beta/2) \|g - h\|^2. \right. \quad (27)$$

which can be alternately written as  $\Pi_{B_c}(h - \frac{1}{\beta} \nabla \eta(h))$ . Implementing a simple quadratic oracle is essentially a projected gradient descent step with a step-size of  $1/\beta$ . The parameter  $\beta$  is a hyper parameter of the quadratic oracle, it is generally taken as the inverse of smoothness constant in canonical gradient descent scheme. It must be emphasised that the actual ‘‘step’’ taken in FLIPS is not this, but in the exact line search.

(ii) *Accelerated Quadratic Oracle*: Adding momentum/acceleration in gradient descent schemes tremendously improves their convergence speeds, both in theory and practice [25]. Taking inspiration from such ideas, the accelerated quadratic oracle is taken as

$$\begin{cases} g(h) = \Pi_{B_c} \left( h - (1/\beta) (\nabla \eta(h) + \rho d) \right), \\ d^+ = g(h) - h. \end{cases} \quad (28)$$

The extra iterate  $d$  is the direction in which the last update was made and must be recursively updated. The parameter  $\rho$  controls the weight of the momentum, and is an additional hyper parameter of the accelerated oracle.

### 3.2. Step size selection via exact line search

Reformulation of problem (1) into problem (14) allows us to compute the explicit solution of the optimal step size without a significant increase in the computational complexity. Given any  $d \in \mathbb{H}$ , let  $h_\gamma := h + \gamma d$  for  $\gamma \in [0, 1]$ . The exact line search problem for a given direction  $d$  and  $\bar{\epsilon} > 0$  is the following scalar optimization problem

$$\gamma(h) = \begin{cases} \operatorname{argmin}_{\gamma \in [0, 1]} & \eta(h_\gamma) = \eta(h + \gamma d) \\ \text{subject to} & h_\gamma \in \mathcal{K}(\bar{\epsilon}). \end{cases} \quad (29)$$

For FLIPS in particular, we consider (29) with  $d = g(h) - h$ , and  $\bar{\epsilon} \in (0, \epsilon)$  such that  $e(f^*) \leq \bar{\epsilon}^2$ .

**Proposition 18.** *The optimal stepsize in the exact line search problem (29) is given by*

$$\gamma(h) = \begin{cases} 0 & \text{if } \left. \frac{\partial \eta(h_\gamma)}{\partial \gamma} \right|_{\gamma=0} \geq 0, \\ \hat{\gamma}(h) & \text{if } \left. \frac{\partial \eta(h_\gamma)}{\partial \gamma} \right|_{\gamma=\hat{\gamma}(h)} \leq 0, \\ \max \left\{ \frac{-s \pm \sqrt{s^2 - 4ru}}{2r} \right\} & \text{otherwise.} \end{cases} \quad (30)$$

where  $\hat{\gamma}(h) := \max \{ \gamma \in [0, 1] : h_\gamma \in \mathcal{K}(\bar{\epsilon}) \}$  and is explicitly characterized in Lemma 31 and the scalars  $s, r, u$  in (31).<sup>4</sup>

---

4

$$\begin{aligned} r &= \|\phi(d)\|^2 (\bar{\epsilon}^2 - e(d)) \\ s &= 2 \langle x, \phi(h) \rangle \langle x, \phi(d) \rangle - (\|x\|^2 - \bar{\epsilon}^2) \langle \phi(h), \phi(d) \rangle \\ u &= \frac{2 \langle x, \phi(d) \rangle \langle x, \phi(h) \rangle \langle \phi(h), \phi(d) \rangle}{\|\phi(d)\|^2} - \frac{\|\phi(h)\|^2 \langle x, \phi(d) \rangle^2}{\|\phi(d)\|^2} - \frac{(\|x\|^2 - \bar{\epsilon}^2) \langle \phi(h), \phi(d) \rangle^2}{\|\phi(d)\|^2}. \end{aligned} \quad (31)$$

### 3.3. Other discussion on FLIPS

**Remark 19** (Stopping criteria). For FLIPS with linear, and the simple quadratic oracle, explicit stopping criteria are proposed.

- (1) Stop if  $g(h) = h$ . In that case, the descent direction remains zero, i.e.,  $d(h) = g(h) - h = 0$ . Therefore, the update on  $h$  is converged,  $h^+ = h + \gamma \cdot 0 = h$ .
- (2) Stop if  $\gamma(h) = 0$ . In this case, regardless of the descent direction, the update will remain the same since  $h^+ = h + 0 \cdot d(h) = h$ .

For the accelerated quadratic oracle, both of the criteria mentioned can occur while the iterate still not being optimal yet due to the momentum, wherein, we typically ran FLIPS for a fixed number of iterations since the iterates converged to the optimal solutions within a few iterations (for example, see Figure 4).

**Remark 20** (Techniques for speeding up implementation of FLIPS). The most computationally demanding aspect of each iteration is computing the matrix vector products  $\phi(h)$  and  $\phi^a(\lambda(h))$  (needed to compute the gradient  $\nabla\eta(h)$ ). Both of these can be addressed, firstly, by observing that computing the product  $\phi(h)$  is only required to compute the inner product  $\langle x, \phi(h) \rangle$ , it is much easier to compute  $\langle \phi^a(x), h \rangle$ . Thus completely avoiding the computation of matrix vector product  $\phi(h)$  since  $\phi^a(x)$  needs to be computed only once. Similar trick can be used to compute the innerproducts  $\langle x, \phi(d) \rangle$  and  $\langle \phi(h), \phi(d) \rangle$  in the exact line search, which then reduces to simply solving a scalar problem.

Secondly, using the expression for  $\lambda(h)$  from (34), we also see that once the quantity  $\phi^a(x)$  is known, it is only required to compute  $(\phi^a \circ \phi)(h)$  which could be much easier since either  $h$  is typically sparse or the operator  $(\phi^a \circ \phi)$  is easy to deal with. In fact for image denoising problems with a unitary dictionary like the DCT matrix, the operator  $(\phi^a \circ \phi)$  is identity.

## 4. NUMERICAL RESULTS

We test FLIPS and compare it with existing methods, by applying them to the image denoising problems. The task is to reconstruct a noisy image (obtained by adding Gaussian noise to its noise-free version). We consider the ‘cameraman’ image of size  $200 \times 200$  on which Gaussian noise of variance is  $\sigma = 0.0055$  is added with the MATLAB function `imnoise`. The image is denoised by individually denoising every patch of a fixed size and then each pixel of the image is reconstructed by taking its average over all the patches it belong to. The experiment is repeated with different patch sizes. For a given patch of size  $m \times m$ , the corresponding denoising problem corresponds to solving the LIP (1) with  $c(f) = \|f\|_1$ , the linear map  $\phi$  as the 2d-inverse discrete cosine transform computed using the function `idct2` in Matlab, and  $\epsilon = \sqrt{\sigma m}$ . All experiments were run on a laptop with Apple M1 Pro and 16GB RAM using MATLAB 2022a. The open-source code can be found on the author’s Github page [21].

**Experiments for FLIPS.** For all the experiments FLIPS was implemented with an accelerated quadratic oracle with the momentum parameter  $\rho = 0.7$ , and the parameter  $\beta$  such that  $(1/\beta) = 1.6 \times 10^{-3}$  (for  $16 \times 16$  patches),  $(1/\beta) = 2.8 \times 10^{-3}$  (for  $32 \times 32$  patches). The experiments to tune parameters for FLIPS (and other methods) are reported in the appendix of this article. The reconstruction results done with a patch size of  $16 \times 16$  are presented in Figure 2, and ones with a patch size of  $32 \times 32$  are presented in Figure 3.



FIGURE 2. From left to right, the original image, the noisy image (PSNR = 22.8829 dB), and the recovered image (PSNR = 28.0921 dB). The image is denoised by applying FLIPS to solve the corresponding LIP for  $16 \times 16$  sliding image patches for 50 iterations.



FIGURE 3. From left to right, the original image, the noisy image (PSNR = 22.8829 dB), and the recovered image (PSNR = 27.6668 dB). The image is denoised by applying FLIPS to solve the corresponding LIP for  $32 \times 32$  sliding image patches for 50 iterations.

**Comparison with existing methods.** We compare FLIPS with the two existing methods as mentioned in the introduction of this paper; the Chambolle-Pock (CP) algorithm [10] and the C-SALSA [1]. For comparison, we consider the same image denoising problems as in Figures 2 and 3 with varying patch sizes.

We implement FLIPS with an accelerated oracle with  $\rho = 0.7$ , and  $\beta^{-1} = 8 \cdot 10^{-2}$  (for  $4 \times 4$ ),  $\beta^{-1} = 2 \cdot 10^{-3}$  (for  $8 \times 8$ ),  $\beta^{-1} = 1.6 \cdot 10^{-3}$  (for  $16 \times 16$ ),  $\beta^{-1} = 2.8 \cdot 10^{-4}$  (for  $32 \times 32$ ),  $\beta^{-1} = 2.8 \cdot 10^{-5}$  (for  $64 \times 64$ ). For C-SALSA, the augmented Lagrangian penalty parameter  $\mu$  is chosen to be 2.5 for all but the case of  $64 \times 64$ ; and for  $64 \times 64$  patches we select  $\mu = 3$ . For CP, the momentum parameter  $\theta = 0.6$  for all the experiments.

Figure 4 shows the iteration by iteration evolution of the image under the three algorithms for the denoising problem solved with  $8 \times 8$  patch sizes. Observe that the image reconstructed by FLIP after only a couple of iterations is already closer to the final reconstruction. For an overall comparison, the average number of iterations (taken over all patches of a fixed size) needed for convergence is tabulated in Table 1. Convergence is decided if the iterates satisfy  $\|f_k - f^*\| \leq 5 \cdot 10^{-3}$ . Since all the three methods solve the LIP (1) using different reformulations, comparing their sub-optimality is not meaningful, and therefore, the comparison is done on the metric of distance to optimal solution  $\|f_k - f^*\|$ .

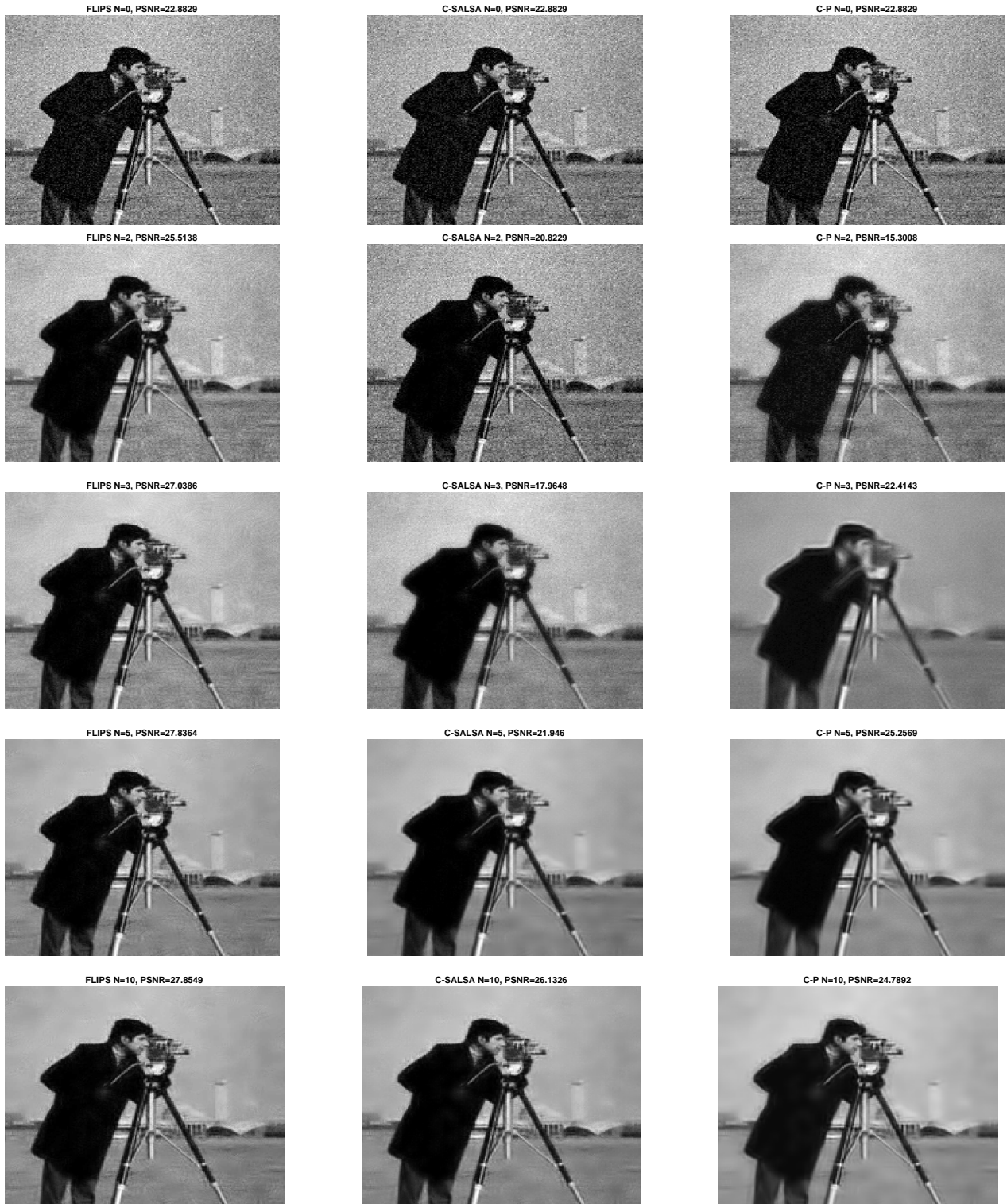


FIGURE 4. Iteration by iteration evolution of the noisy image under FLIPS, C-SALSA, and CP denoised with  $8 \times 8$  sliding patch approach.



TABLE 1. Average number of iterations needed till convergence for CP, C-SALSA, and FLIPS for the denoising problem with varying patch sizes.

	$4 \times 4$	$8 \times 8$	$16 \times 16$	$32 \times 32$	$64 \times 64$
<b>CP</b>	58.1	44.9	46.1	51.3	47.3
<b>C-SALSA</b>	21.1	22.3	22.8	22.1	18.2
<b>FLIPS</b>	6.0	8.7	9.8	13.9	11.3

#### 4.1. Results for a single patch

To highlight further aspect of FLIPS and its comparison with other methods, we focus on convergence plots for a single  $32 \times 32$  patch (shown in Figure 5) extracted from the ‘cameraman’ image.



FIGURE 5. Single  $32 \times 32$  patch of ‘cameraman’ image from Figure 3 used as the input for the experiments in Figures 6, 7a, and 7b.

For  $\beta = 1 \times 10^{-5}$  in FLIPS, the plots for sub-optimality:  $\eta(h_k) - c^*$ , distance to optimal solution  $\|f_k - f^*\|$ , and the plot for step-size sequence  $\gamma_k$  are presented in Figure 6. By choosing a different value of  $\beta = 1 \times 10^{-5}$  (other than the value of  $2.8 \times 10^{-5}$ ), we see that the performance of FLIPS improves further significantly. This is because the parameter of FLIPS are tuned for average convergence of all patches (which are mostly constant value patches in the cameraman image). Whereas, the patch in Figure 5 is atypical.

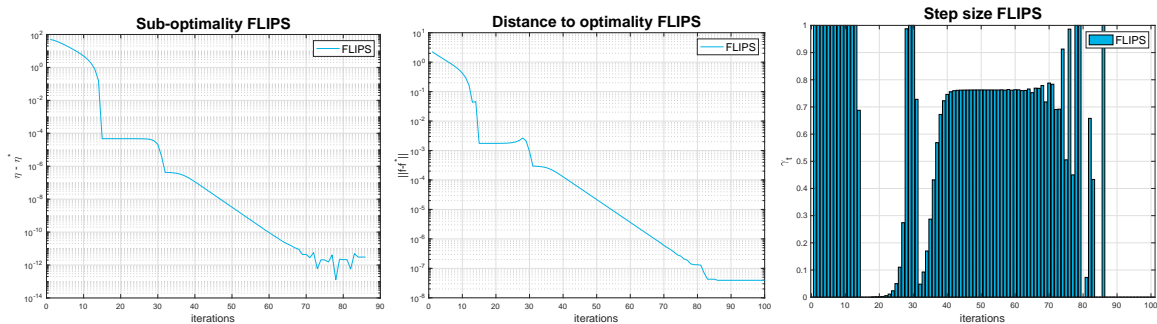
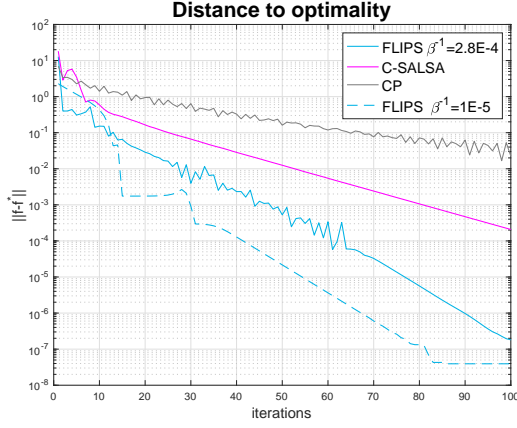


FIGURE 6. From left to right: the sub-optimality  $\eta(h_k) - c^*$ , and the distance to optimal solution  $\|f - f^*\|$ , and the step size sequence  $(\gamma_k)_k$  in FLIPS for the denoising experiment of a single  $32 \times 32$  (shown in Figure 5).

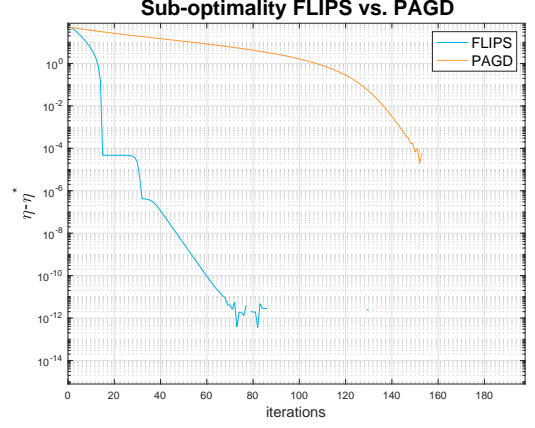
For comparison, keeping the same parameters as in the experiment for Figure 3, we highlight in Figure 7a that FLIPS converges faster than both C-SALSA and CP. More importantly, for both choices of the parameter  $\beta$ . Then in Figure 7b, we compare the sub-optimality  $\eta(h_k) - c^*$  of iterates generated by FLIPS and the canonical projected accelerated gradient descent (PAGD) as in (19) (applied with  $(1/b) = 2.2 \cdot 10^{-6}$  after tuning). Figure 7b clearly shows that FLIPS outperforms PAGD in terms of convergence.

#### 4.2. Empirical validation for choosing $\bar{\epsilon}$ (Remark 6)





(A) Comparison of FLIPS with C-SALSA and CP.



(B) Comparison of FLIPS with projected accelerated GD.

FIGURE 7. Comparison of FLIPS with other methods on the single  $32 \times 32$  patch shown in Figure 5.

To empirically validate Remark 6, an experiment was conducted to check if  $e(f^*) < \bar{\epsilon}^2$  by a margin. From the full  $200 \times 200$  image, 28561 different  $32 \times 32$  patches were extracted and the corresponding LIPs were solved to obtain the optimal solution  $f^*$  for each plot. Then the histogram of values  $e(f^*)$  collected for all 28561 patches is plotted in Figure 8 (with a bandwidth of 0.01). It can be seen that there is a clear gap between the maximum  $e(f^*)$  and  $\bar{\epsilon}^2$ . Thus, verifying empirically Remark 6.

## 5. TECHNICAL PROOFS

**Proposition 21.** *Let  $x, \phi$ , and  $\epsilon$  be such that Assumption 2 holds. For any  $h \in B_c$ , considering the maximization problem*

$$\left\{ \sup_{\lambda \in \Lambda} L(\lambda, h) := 2l(\lambda) - \langle \lambda, \phi(h) \rangle, \right. \quad (32)$$

*the following assertions hold.*

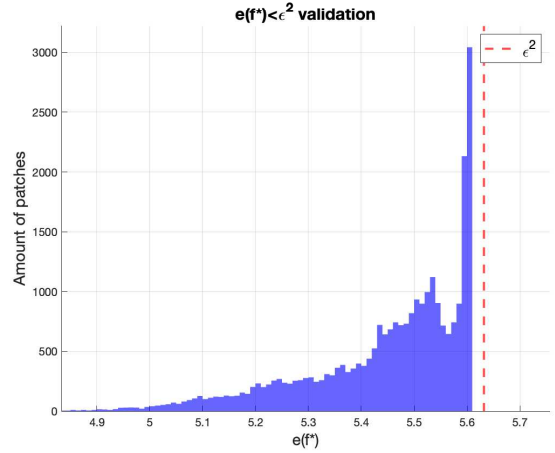
- (i) *The maximization problem (32) is bounded if and only if  $h \in \mathcal{K}(\epsilon)$ , and the maximal value is equal to  $\eta(h)$ . In other words,*

$$\eta(h) = \sup_{\lambda \in \Lambda} L(\lambda, h) \quad \text{for all } h \in \mathcal{K}(\epsilon). \quad (33)$$

- (ii) *The maximization problem (32) admits a unique maximizer  $\lambda(h)$  if and only if  $h \in \text{int}(\mathcal{K}(\epsilon)) = \{h \in \mathbb{H} : \langle x, \phi(h) \rangle > 0, \text{ and } e(h) < \epsilon^2\}$ , which is given by*

$$\lambda(h) = \frac{\eta(h)}{\|\phi(h)\| \sqrt{\epsilon^2 - e(h)}} (x - \eta(h) \phi(h)). \quad (34)$$

The proof of Proposition 21 relies heavily on [22, Lemma 35, 36] under the setting  $r = 2, q = 0.5$ , and  $\delta = 0$ . We shall first provide three lemmas from which Proposition 21 follows easily.

FIGURE 8. Histogram of the values of  $e(f^*)$  for all  $32 \times 32$  patches of the 'cameraman image' from Figure

**Lemma 22** (Unboundedness in (32)). *The maximization problem (32) is unbounded for  $h \notin \mathcal{K}(\epsilon)$ .*

*Lemma 22.* We first recall from [22, Lemma 36 and assertion (iii) of Lemma 35] that the maximal value of (32) is unbounded if and only if there exists a  $\lambda'$  such that the two following inequalities are satisfied simultaneously

$$\langle \lambda', \phi(h) \rangle \leq 0 < \langle \lambda', x \rangle - \epsilon \|\lambda'\|. \quad (35)$$

Since  $h \notin \mathcal{K}(\epsilon)$ , either  $\langle x, \phi(h) \rangle < 0$  or  $e(h) > \epsilon^2$ . On the one hand, if  $\langle x, \phi(h) \rangle < 0$ , then we observe that  $\lambda' = x$  satisfies the two inequalities of (35) since  $\|x\| > \epsilon$ . On the other hand, if  $e(h) > \epsilon^2$ , then by considering  $\lambda' = x - \frac{\langle x, \phi(h) \rangle}{\|\phi(h)\|^2} \phi(h)$ , we first observe that  $\langle \lambda', \phi(h) \rangle = 0$ , and by Pythagoras theorem, we have  $\|\lambda'\|^2 = e(h)$ . It is now easily verified that  $\lambda'$  satisfies the two inequalities (35) simultaneously since

$$\begin{cases} \langle \lambda', \phi(h) \rangle = \langle x, \phi(h) \rangle - \frac{\langle x, \phi(h) \rangle}{\|\phi(h)\|^2} \langle \phi(h), \phi(h) \rangle = 0 \\ \langle \lambda', x \rangle - \epsilon \|\lambda'\| = \|x\|^2 - \frac{|\langle x, \phi(h) \rangle|^2}{\|\phi(h)\|^2} - \epsilon \sqrt{e(h)} = \sqrt{e(h)}(\sqrt{e(h)} - \epsilon) > 0. \end{cases}$$

Thus the lemma holds.  $\square$

**Lemma 23** (Optimal value of (32)). *If  $h \in \mathcal{K}(\epsilon)$ , then the maximal value of (32) is finite and equal to  $\eta(h)$  (as in (8)).*

*Lemma 23.* We now recall from [22, Lemma 36, and (51)-Lemma 35], that the maximal value of (32) is bounded if and only if the following minimum exists

$$\min \{ \theta \geq 0 : \|x - \theta \phi(h)\| \leq \epsilon \}. \quad (36)$$

Clearly, the minimum in (36) exists whenever the minimization problem is feasible. Suppose there exists some  $\theta' \geq 0$  such that  $\|x - \theta' \phi(h)\| \leq \epsilon$ , it is immediately seen that

$$\begin{cases} \langle x, \phi(h) \rangle \geq \frac{1}{2\theta'} \left( (\|x\|^2 - \epsilon^2) + \theta'^2 \|\phi(h)\|^2 \right) > 0, \text{ and} \\ e(h) = \min_{\theta \in \mathbb{R}} \|x - \theta \phi(h)\|^2 \leq \|x - \theta' \phi(h)\|^2 \leq \epsilon^2. \end{cases}$$

Thus,  $h \in \mathcal{K}(\epsilon)$ . On the contrary, if  $h \notin \mathcal{K}(\epsilon)$ , then it also seen similarly that  $\theta' = \frac{\langle x, \phi(h) \rangle}{\|\phi(h)\|^2}$  is feasible for (36). Thus, the maximal value of (32), and the minimum in (36) is finite if and only if  $h \in \mathcal{K}(\epsilon)$ .

It is immediately realised that the value of the minimum in (36) corresponds to the smaller root of the quadratic equation  $\|x - \theta \phi(h)\|^2 = \epsilon^2$ . Dividing throughout therein by  $\theta^2$ , we obtain a different quadratic equation

$$\frac{1}{\theta^2} (\|x\|^2 - \epsilon^2) - \frac{2}{\theta} \langle x, \phi(h) \rangle + \|\phi(h)\|^2 = 0.$$

Selecting the larger root (and hence smaller  $\theta$ ) gives us that for every  $h \in \mathcal{K}(\epsilon)$ , the optimal value of (32) (and (36)) is

$$\frac{\|x\|^2 - \epsilon^2}{\langle x, \phi(h) \rangle + \|\phi(h)\| \sqrt{\epsilon^2 - e(h)}} = \eta(h).$$

Alternatively, if one selects the smaller root of the quadratic equation  $\|x - \theta \phi(h)\|^2 = \epsilon^2$ , one gets the expression of eta provided in (38).  $\square$

**Remark 24** (Quadratic equation for  $\eta(h)$ ). It is apparent from the proof of the Lemma 23 that for any  $h \in \mathcal{K}(\epsilon)$ ,  $\eta(h)$  satisfies

$$\|x - \eta(h) \phi(h)\| = \epsilon. \quad (37)$$

For  $h \in \mathcal{K}(\epsilon)$ , since  $\langle x, \phi(h) \rangle \geq 0$ , we see that the quadratic equation  $\|x - \theta\phi(h)\|^2 = \epsilon^2$  has two positive real roots. Moreover,  $\eta(h)$  is the smallest positive root of this quadratic equation, which gives

$$\eta(h) = \frac{\langle x, \phi(h) \rangle - \|\phi(h)\| \sqrt{\epsilon^2 - e(h)}}{\|\phi(h)\|^2} \quad \text{for every } h \in \mathcal{K}(\epsilon). \quad (38)$$

**Lemma 25.** *Suppose,  $\lambda(h)$  is an optimal solution to the maximization problem (32), then it also satisfies*

$$\eta(h) = L(\lambda(h), h) = \sqrt{\langle \lambda(h), x \rangle - \epsilon \|\lambda(h)\|}. \quad (39)$$

*Lemma 25.* First of all, we observe that the maximization problem (32) admits an optimal solution if and only if it satisfies the first order optimality conditions:

$$0 = \frac{\partial}{\partial \lambda} L(\lambda(h), h) = \frac{x - \frac{\epsilon}{\|\lambda(h)\|} \lambda(h)}{\sqrt{\langle \lambda(h), x \rangle - \epsilon \|\lambda(h)\|}} - \phi(h).$$

By taking inner product throughout with  $\lambda(h)$ , it is readily seen that

$$\sqrt{\langle \lambda(h), x \rangle - \epsilon \|\lambda(h)\|} = \langle \lambda(h), \phi(h) \rangle.$$

Thus, we have

$$\begin{aligned} \eta(h) &= L(\lambda(h), h) \quad \text{from Lemma 23,} \\ &= 2\sqrt{\langle \lambda(h), x \rangle - \epsilon \|\lambda(h)\|} - \langle \lambda(h), \phi(h) \rangle \\ &= \sqrt{\langle \lambda(h), x \rangle - \epsilon \|\lambda(h)\|}. \end{aligned}$$

□

*Proof of Proposition 21.* Lemma 22 and 23 together imply assertion (i) of the proposition. To complete the proof of the proposition, it now only remains to be shown that the maximization problem (32) admits a unique optimal solution  $\lambda(h)$  if and only if  $h \in \text{int}(\mathcal{K}(\epsilon))$ .

Firstly, we observe that the maximization problem (32) admits an optimal solution if and only if it satisfies the first order optimality conditions:  $0 = \frac{\partial}{\partial \lambda} L(\lambda(h), h)$ , rearranging terms, we obtain

$$\frac{\epsilon}{\|\lambda(h)\|} \lambda(h) = x - \sqrt{\langle \lambda(h), x \rangle - \epsilon \|\lambda(h)\|} \phi(h) = x - \eta(h) \phi(h),^5 \quad (40)$$

the last equality is due to (39). Now, we observe that any  $\lambda(h)$  that satisfies the implicit non-linear equation (40) must be of the form  $\lambda(h) = r(x - \eta(h) \phi(h))$  for some  $r > 0$ . The precise value of  $r > 0$  can be computed using (39). We have

$$\begin{aligned} \eta(h) &= \sqrt{\langle \lambda(h), x \rangle - \epsilon \|\lambda(h)\|} \\ &= \sqrt{r} \sqrt{\langle x - \eta(h) \phi(h), x \rangle - \epsilon \|x - \eta(h) \phi(h)\|} \\ &= \sqrt{r} \sqrt{\|x - \eta(h) \phi(h)\|^2 + \langle x - \eta(h) \phi(h), \eta(h) \phi(h) \rangle - \epsilon^2} \\ &= \sqrt{r\eta(h)} \sqrt{\langle x, \phi(h) \rangle - \eta(h) \|\phi(h)\|^2}, \end{aligned}$$

from which it is easily picked that  $r = \frac{\langle x, \phi(h) \rangle - \eta(h) \|\phi(h)\|^2}{\|\phi(h)\| \sqrt{\epsilon^2 - e(h)}}$ . Now,  $r > 0$  if and only if  $e(h) < \epsilon^2$ , or equivalently,  $h \in \text{int}(\mathcal{K}(\epsilon))$ . Thus, we finally conclude that the optimality condition

<sup>5</sup>Observe that by evaluating squared norm on both sides of (40) and using (39) also gives rise to the quadratic equation  $\epsilon^2 = \|x - \eta(h) \phi(h)\|^2$  for  $\eta(h)$ .

(40) has a unique solution  $\lambda(h)$  if and only if  $h \in \text{int}(\mathcal{K}(\epsilon))$ , and is given by

$$\lambda(h) = \frac{\eta(h)}{\|\phi(h)\| \sqrt{\epsilon^2 - e(h)}} (x - \eta(h) \phi(h)).$$

The proof of the proposition is complete.  $\square$

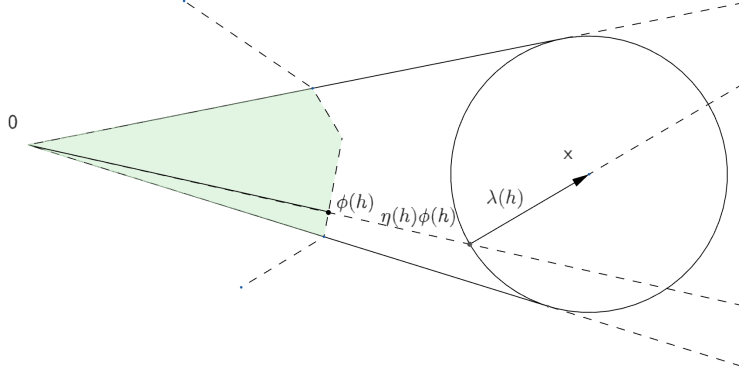


FIGURE 9. Graphical overview of the direction of lambda

**Lemma 26.** For every  $h \in \mathcal{K}(\epsilon)$ , the following relations hold

$$\eta(h) \|\phi(h)\| \geq \|x\| - \epsilon, \quad (41)$$

$$\langle x - \eta(h) \phi(h), \phi(h) \rangle = \|\phi(h)\| \sqrt{\epsilon^2 - e(h)}. \quad (42)$$

*Proof.* For any  $h \in \mathcal{K}(\epsilon)$ , we see from (8) that

$$\begin{aligned} \frac{1}{\eta(h)} &= \frac{\|\phi(h)\|}{(\|x\|^2 - \epsilon^2)} \left( \frac{\langle x, \phi(h) \rangle}{\|\phi(h)\|} + \sqrt{\epsilon^2 - e(h)} \right) \\ &< \frac{\|\phi(h)\|}{(\|x\|^2 - \epsilon^2)} (\|x\| + \epsilon) \quad \text{due to C-S inequality, and } 0 \leq e(h), \\ &= \frac{\|\phi(h)\|}{\|x\| - \epsilon}, \end{aligned}$$

On rearranging terms, the inequality (41) is obtained at once. Similarly, rearranging terms in (37), we see

$$\|\phi(h)\| \sqrt{\epsilon^2 - e(h)} = \langle x, \phi(h) \rangle - \eta(h) \|\phi(h)\|^2,$$

Observing that  $\langle x, \phi(h) \rangle - \eta(h) \|\phi(h)\|^2 = \langle x - \eta(h) \phi(h), \phi(h) \rangle$ , (42) follows immediately.  $\square$

**Lemma 27** (Derivative of  $\lambda(h)$ ). Let  $x, \phi, \epsilon$  be given such that Assumption 2 holds, then the mapping  $\text{int}(\mathcal{K}(\epsilon)) \ni h \mapsto \lambda(h)$  is continuously differentiable. Moreover, with the continuous maps  $\text{int}(\mathcal{K}(\epsilon)) \ni h \mapsto (r(h), M(h)) \in (0, +\infty) \times \mathbb{R}^{n \times n}$  defined as

$$\begin{cases} r(h) := \frac{2\epsilon}{\|\lambda(h)\|} + \frac{(\|x\|^2 - \epsilon^2)}{\eta^2(h)}, \quad \text{and} \\ M(h) := \frac{\|\lambda(h)\|}{\epsilon \eta(h)} \left( \eta^2(h) \mathbb{I}_n + r(h) (\lambda(h) \lambda^\top(h)) - (\lambda(h) x^\top + x \lambda^\top(h)) \right), \end{cases} \quad (43)$$

the derivative of  $h \mapsto \lambda(h)$  is the linear map  $\left( \frac{\partial \lambda(h)}{\partial h} \right) : \mathbb{H} \rightarrow \mathbb{R}^n$  given by

$$\left( \frac{\partial \lambda(h)}{\partial h} \right) (v) = -M(h) \cdot \phi(v) \text{ for all } v \in \mathbb{H}. \quad (44)$$

*Lemma 27.* First, we rewrite (34) as

$$\langle x - \eta(h) \phi(h), \phi(h) \rangle \lambda(h) = \eta(h) (x - \eta(h) \phi(h)),$$

then by differentiating on both sides w.r.t.  $h$ , we obtain an equation in the space of linear operators from  $\mathbb{H}$  to  $\mathbb{R}^n$ . Evaluating the operators on the both sides of this equation at some  $v \in \mathbb{H}$ , we get

$$\begin{aligned} \langle x - \eta(h) \phi(h), \phi(h) \rangle \left( \frac{\partial \lambda(h)}{\partial h} \right) (v) + \left\langle \nabla \left( \langle x - \eta(h) \phi(h), \phi(h) \rangle \right), v \right\rangle \lambda(h) \\ = \langle \nabla \eta(h), v \rangle x - \eta^2(h) \phi(v) - 2\eta(h) \langle \nabla \eta(h), v \rangle \phi(h). \end{aligned} \quad (45)$$

On the one hand, we have

$$\begin{aligned} \langle \nabla \eta(h), v \rangle x - \eta^2(h) \phi(v) - 2\eta(h) \langle \nabla \eta(h), v \rangle \phi(h) \\ = \langle \nabla \eta(h), v \rangle (x - 2\eta(h) \phi(h)) - \eta^2(h) \phi(v) \\ = -\langle \lambda(h), \phi(v) \rangle (x - 2\eta(h) \phi(h)) - \eta^2(h) \phi(v) \quad \text{since } \nabla \eta(h) = -\phi^\alpha(\lambda(h)) \\ = -\left( \eta^2(h) \mathbb{I}_n + (x - 2\eta(h) \phi(h)) \lambda^\top(h) \right) \cdot \phi(v) \\ = -\left( \eta^2(h) \mathbb{I}_n + (-x + 2\epsilon/\|\lambda(h)\| \lambda(h)) \lambda^\top(h) \right) \cdot \phi(v) \\ = -\left( \eta^2(h) \mathbb{I}_n + 2\epsilon/\|\lambda(h)\| (\lambda(h) \lambda^\top(h)) - (x \lambda^\top(h)) \right) \cdot \phi(v). \end{aligned} \quad (46)$$

On the other hand, since

$$\begin{aligned} \nabla \left( \langle x - \eta(h) \phi(h), \phi(h) \rangle \right) &= \phi^\alpha(x) - 2\eta(h) \phi^\alpha(\phi(h)) - \|\phi(h)\|^2 \nabla \eta(h) \\ &= \phi^\alpha \left( x - 2\eta(h) \phi(h) + \|\phi(h)\|^2 \lambda(h) \right), \end{aligned}$$

we also have

$$\begin{aligned} \left\langle \nabla \left( \langle x - \eta(h) \phi(h), \phi(h) \rangle \right), v \right\rangle \lambda(h) \\ = \left\langle (x - 2\eta(h) \phi(h) + \|\phi(h)\|^2 \lambda(h)), \phi(v) \right\rangle \lambda(h) \\ = \left( \lambda(h) (x - 2\eta(h) \phi(h) + \|\phi(h)\|^2 \lambda(h))^\top \right) \cdot \phi(v) \\ = \left( \lambda(h) (-x + (2\epsilon/\|\lambda(h)\| + \|\phi(h)\|^2) \lambda(h))^\top \right) \cdot \phi(v) \quad \text{from (34)} \\ = \left( -(\lambda(h) x^\top) + (2\epsilon/\|\lambda(h)\| + \|\phi(h)\|^2) (\lambda(h) \lambda^\top(h)) \right) \cdot \phi(v). \end{aligned} \quad (47)$$

Collecting (46) and (47), together with  $\langle x - \eta(h) \phi(h), \phi(h) \rangle = \frac{\epsilon \eta(h)}{\|\lambda(h)\|}$  (from (34)), (45) simplifies to reveal

$$\begin{aligned} \frac{\epsilon \eta(h)}{\|\lambda(h)\|} \left( \frac{\partial \lambda(h)}{\partial h} \right) (v) &= -\left( \eta^2(h) \mathbb{I}_n - (x \lambda^\top(h) + \lambda(h x^\top)) \right) \cdot \phi(v) \\ &\quad - \left( 4\epsilon/\|\lambda(h)\| + \|\phi(h)\|^2 \right) (\lambda(h) \lambda^\top(h)) \cdot \phi(v). \end{aligned}$$

Finally, simplifying

$$\begin{aligned} \frac{2\epsilon}{\|\lambda(h)\|} + \|\phi(h)\|^2 &= \frac{2\langle x - \eta(h) \phi(h), \phi(h) \rangle}{\eta(h)} + \|\phi(h)\|^2 \quad \text{from (34)} \\ &= \frac{2\langle x, \phi(h) \rangle}{\eta(h)} - \|\phi(h)\|^2 \\ &= \frac{1}{\eta^2(h)} \left( 2\langle x, \eta(h) \phi(h) \rangle - \eta^2(h) \|\phi(h)\|^2 \right) \\ &= \frac{1}{\eta^2(h)} \left( \|x\|^2 - \|x - \eta(h) \phi(h)\|^2 \right) = \frac{(\|x\|^2 - \epsilon^2)}{\eta^2(h)}. \end{aligned}$$

Putting everything together, the derivative  $\left(\frac{\partial\lambda(h)}{\partial h}\right)(v)$  is easily written in terms of the matrix  $M(h)$  given in (43) as

$$\left(\frac{\partial\lambda(h)}{\partial h}\right)(v) = M(h) \cdot \phi(v)$$

Continuous differentiability of  $\text{int}(\mathcal{K}(\epsilon)) \ni h \mapsto \lambda(h) \in \mathbb{R}^n$  follows directly from continuity of the map  $\text{int}(\mathcal{K}(\epsilon)) \ni h \mapsto M(h) \in \mathbb{R}^{n \times n}$ , which is straight forward. The proof of the lemma is complete.  $\square$

*Proof of Proposition 3.* From assertion (i) of Proposition 21, it is inferred that for every  $h \in \mathcal{K}(\epsilon)$ , the value  $\eta(h)$  is a point-wise maximum of the linear function  $L(\lambda, h)$  (linear in  $h$ ). Thus, the mapping  $\eta : \mathcal{K}(\epsilon) \rightarrow [0, +\infty)$  is convex.

From assertion (ii) of Proposition 21, it follows that the maximization problem (32) admits a solution  $\lambda(h)$  if and only if  $h \in \mathcal{K}(\bar{\epsilon})$ . Then, from Danskin's theorem [4], we conclude that the function  $\eta : \mathcal{K}(\epsilon) \rightarrow [0, +\infty)$  is differentiable if and only if the maximizer  $\lambda(h)$  in (32) exists. Thus,  $\eta : \mathcal{K}(\epsilon) \rightarrow [0, +\infty)$  is differentiable at every  $h \in \text{int}(\mathcal{K}(\epsilon))$ , and the derivative is given by  $\nabla\eta(h) = -\phi^a(\lambda(h))$ . Substituting for  $\lambda(h)$  from (34), we immediately get (9).

Since  $\nabla\eta(h) = -\phi^a(\lambda(h))$ , we realise that  $\eta(h)$  is twice differentiable if and only if the mapping  $h \mapsto \lambda(h)$  has a well-defined derivative  $\left(\frac{\partial\lambda(h)}{\partial h}\right)$ . In which case, the hessian is a linear operator  $(\Delta^2\eta(h)) : \mathbb{H} \rightarrow \mathbb{H}$  given by

$$(\Delta^2\eta(h))(v) = -\phi^a \circ \left(\frac{\partial\lambda(h)}{\partial h}\right)(v) \quad \text{for all } v \in \mathbb{H}.$$

We know that the derivative  $\left(\frac{\partial\lambda(h)}{\partial h}\right)$  exists for every  $h \in \text{int}(\mathcal{K}(\epsilon))$ , thus,  $\eta(\cdot)$  is twice differentiable everywhere on  $\text{int}(\mathcal{K}(\epsilon))$ . Substituting for  $\left(\frac{\partial\lambda(h)}{\partial h}\right)$  from (44), we immediately get

$$(\Delta^2\eta(h))(v) = (\phi^a \circ M(h) \circ \phi)(v) \quad \text{for all } v \in \mathbb{H},$$

where  $h \mapsto M(h)$  is a matrix valued map given in (43). Moreover, continuity of the hessian i.e., continuity of the map  $\text{int}(\mathcal{K}(\epsilon)) \ni h \mapsto (\Delta^2\eta(h))$  follows directly from the continuity of  $\text{int}(\mathcal{K}(\epsilon)) \ni h \mapsto \left(\frac{\partial\lambda(h)}{\partial h}\right)$ . The proof is now complete.  $\square$

**Lemma 28** (Smallest and largest eigenvalues of  $M(h)$ ). *For every  $h \in \text{int}(\mathcal{K}(\epsilon))$ , consider  $M(h) \in \mathbb{R}^{n \times n}$  as given in (43). Then its minimum and maximum eigenvalues, denoted by  $\bar{\sigma}(M(h))$  and  $\hat{\sigma}(M(h))$  respectively, are*

$$\begin{cases} \bar{\sigma}(M(h)) = \frac{(\|x\|^2 - \epsilon^2) \|\lambda(h)\|^3}{2\epsilon\eta^3(h)} \left(1 - \sqrt{1 - \frac{8\epsilon\eta^6(h)}{(\|x\|^2 - \epsilon^2)^2 \|\lambda(h)\|^3}}\right) \\ \hat{\sigma}(M(h)) = \frac{(\|x\|^2 - \epsilon^2) \|\lambda(h)\|^3}{2\epsilon\eta^3(h)} \left(1 + \sqrt{1 - \frac{8\epsilon\eta^6(h)}{(\|x\|^2 - \epsilon^2)^2 \|\lambda(h)\|^3}}\right). \end{cases} \quad (48)$$

*Lemma 28.* Recall from (43) that

$$\begin{cases} r(h) = \frac{2\epsilon}{\|\lambda(h)\|} + \frac{(\|x\|^2 - \epsilon^2)}{\eta^2(h)}, \quad \text{and} \\ M(h) = \frac{\|\lambda(h)\|}{\epsilon\eta(h)} \left( \eta^2(h) \mathbb{I}_n + r(h) (\lambda(h)\lambda^\top(h) - (\lambda(h)x^\top + x\lambda^\top(h))) \right). \end{cases}$$

First, suppose that  $\lambda(h)$  and  $x$  are linearly independent. Then it is clear that the subspace  $S := \text{span}\{\lambda(h), x\}$  is invariant under the linear transformation given by the matrix  $M(h)$ , and this linear transformation is identity on the orthogonal complement of  $S$ . Then it is also evident that the hessian has  $n - 2$  eigenvalues equal to  $(1/\epsilon)\eta(h)\|\lambda(h)\|$  and the two other distinct eigenvalues corresponding to the restriction of  $M(h)$  onto the 2-dimensional subspace  $S$ .

Let  $T$  denote the  $2 \times 2$  matrix representing the restriction of  $M(h)$  onto the subspace  $S$  for  $\{\lambda(h), x\}$  being chosen as a basis for  $S$ . In other words, it holds that  $M(h)[x \ \lambda(h)] = [x \ \lambda(h)]T$ . Using the fact that  $\eta^2(h) = \langle \lambda(h), x \rangle - \epsilon \|\lambda(h)\|$  from (39), it is easily verified that the matrix  $T$  simplifies to

$$T = \frac{\|\lambda(h)\|}{\epsilon \eta(h)} \begin{pmatrix} -\epsilon \|\lambda(h)\| & -\|\lambda(h)\|^2 \\ r(h) \langle \lambda(h), x \rangle - \|x\|^2 & r(h) \|\lambda(h)\|^2 - \epsilon \|\lambda(h)\| \end{pmatrix}. \quad (49)$$

Furthermore, substituting  $r(h)$ , it is also verified that  $\text{tr}(T) = \frac{\|\lambda(h)\|^2}{\eta^2(h)} (\|x\|^2 - \epsilon^2)$  and  $\det(T) = 2\epsilon \eta^2(h) \|\lambda(h)\|$ . Now, it is easily verified that the two eigenvalues of  $T$  are precisely equal to  $\{\bar{\sigma}(M(h)), \hat{\sigma}(M(h))\}$ .

Since apart from  $\{\bar{\sigma}(M(h)), \hat{\sigma}(M(h))\}$ , the rest of the eigenvalues of  $M(h)$  are equal to  $\frac{1}{\epsilon} \eta(h) \|\lambda(h)\|$ , it remains to be shown that  $\bar{\sigma}(M(h)) \leq \frac{1}{\epsilon} \eta(h) \|\lambda(h)\| \leq \hat{\sigma}(M(h))$ ; which we do so by producing  $u_1, u_2 \in S$  such that

$$\bar{\sigma}(M(h)) \leq \frac{\langle u_1, M(h)u_1 \rangle}{\|u_1\|^2} \leq \frac{1}{\epsilon} \eta(h) \|\lambda(h)\| \leq \frac{\langle u_2, M(h)u_2 \rangle}{\|u_2\|^2} \leq \hat{\sigma}(M(h)). \quad (50)$$

Observe that the inequalities  $\bar{\sigma}(M(h)) \leq \frac{\langle u_1, M(h)u_1 \rangle}{\|u_1\|^2}$ , and  $\frac{\langle u_2, M(h)u_2 \rangle}{\|u_2\|^2} \leq \hat{\sigma}(M(h))$  readily hold for any  $u_1, u_2 \in S$  since  $\bar{\sigma}(M(h)), \hat{\sigma}(M(h))$  are the two eigenvalues of  $M(h)$  when restricted to the subspace  $S$ . To obtain the rest of the inequalities in (50), consider

$$u_1 = x + \frac{\|x\|^2 - r(h) \langle \lambda(h), x \rangle}{r(h) \|\lambda(h)\|^2 - \langle \lambda(h), x \rangle} \lambda(h) \quad \text{and} \quad u_2 = x - \frac{\|x\|^2}{\langle \lambda(h), x \rangle} \lambda(h).$$

It is easily verified that  $\langle u_1, r(h)\lambda(h) - x \rangle = 0$  and  $\langle u_2, x \rangle = 0$ . Moreover, rewriting  $M(h)$  by completing squares as

$$M(h) = \frac{\|\lambda(h)\|}{\epsilon r(h) \eta(h)} \left( \eta^2(h) r(h) \mathbb{I}_n + (r(h)\lambda(h) - x)(r(h)\lambda(h) - x)^\top - x x^\top \right),$$

it is also easily verified that the inequalities

$$\begin{cases} \frac{\langle u_1, M(h)u_1 \rangle}{\|u_1\|^2} = \frac{\|\lambda(h)\|}{\epsilon r(h) \eta(h)} \left( \eta^2(h) - \frac{|\langle u_1, x \rangle|^2}{\|u_1\|^2} \right) & \leq \frac{1}{\epsilon} r(h) \|\lambda(h)\|, \\ \frac{\langle u_2, M(h)u_2 \rangle}{\|u_2\|^2} = \frac{\|\lambda(h)\|}{\epsilon r(h) \eta(h)} \left( \eta^2(h) + \frac{|\langle u_2, r(h)\lambda(h) - x \rangle|^2}{\|u_2\|^2} \right) & \geq \frac{1}{\epsilon} r(h) \|\lambda(h)\|. \end{cases}$$

Thus, the inequalities (50) are obtained at once.

To complete the proof for the case when  $\lambda(h)$  and  $x$  are linearly dependent, we first see that the  $\text{int}(\mathcal{K}(\epsilon)) \ni h \mapsto (\bar{\sigma}(M(h)), \hat{\sigma}(M(h)))$  is continuous. Secondly, since the mapping  $\text{int}(\mathcal{K}(\epsilon)) \ni h \mapsto M(h)$  is also continuous, and the eigenvalues of a matrix vary continuously, these two limits must be the same. The proof is now complete.  $\square$

*Proof of Proposition 4.* For any  $\bar{\epsilon} \in (0, \epsilon)$  and  $\hat{\eta} > c^*$ , we know that the set  $\mathcal{H}(\bar{\epsilon}, \hat{\eta}) \subset \text{int}(\mathcal{K}(\epsilon))$ . Consequently, it follows from Proposition 3 that  $\eta : \mathcal{H}(\bar{\epsilon}, \hat{\eta}) \rightarrow [0, +\infty)$  is twice continuously differentiable. To establish the required smoothness, and strong convexity assertions of the proposition, we first obtain uniform upper (lower) bound on the maximum (minimum) eigenvalue of the Hessian  $(\Delta^2 \eta(h))$ . To this end, for every  $v \in \mathbb{H}$ , since  $\langle v, (\Delta^2 \eta(h))(v) \rangle = \langle \phi(v), M(h)\phi(v) \rangle$ , we see that

$$\bar{\sigma}(M(h)) \bar{\sigma}(\phi^a \circ \phi) \leq \frac{\langle v, (\Delta^2 \eta(h))(v) \rangle}{\|v\|^2} \leq \hat{\sigma}(M(h)) \hat{\sigma}(\phi^a \circ \phi) \quad \text{for all } v \in \mathbb{H}. \quad (51)$$

The quantities  $\bar{\sigma}(\phi^a \circ \phi)$  and  $\hat{\sigma}(\phi^a \circ \phi)$  are the minimum and maximum eigenvalues of the linear operator  $\phi^a \circ \phi : \mathbb{H} \rightarrow \mathbb{H}$  respectively. Denoting  $\hat{\sigma}(\Delta^2 \eta(h))$  and  $\bar{\sigma}(\Delta^2 \eta(h))$  to be the the maximum and minimum eigenvalues of the hessian respectively, it follows from (51) that

$$\bar{\sigma}(M(h)) \bar{\sigma}(\phi^a \circ \phi) \leq \bar{\sigma}(\Delta^2 \eta(h)) \leq \hat{\sigma}(\Delta^2 \eta(h)) \leq \hat{\sigma}(M(h)) \hat{\sigma}(\phi^a \circ \phi). \quad (52)$$



**Uniform upper bound for  $\hat{\sigma}(M(h))$ .** For every  $h \in \mathcal{H}(\bar{\epsilon}, \hat{\eta}) \subset \mathcal{H}$ , we have the inequality

$$\begin{aligned} \frac{\|\lambda(h)\|}{\eta(h)} &= \frac{\|x - \eta(h)\phi(h)\|}{\|\phi(h)\| \sqrt{\epsilon^2 - e(h)}} = \frac{\epsilon}{\|\phi(h)\| \sqrt{\epsilon^2 - e(h)}}, \text{ from (37),} \\ &< \frac{\epsilon}{\|\phi(h)\| \sqrt{\epsilon^2 - \bar{\epsilon}^2}}, \text{ since } e(h) < \bar{\epsilon}^2 \text{ for } h \in \mathcal{H}(\bar{\epsilon}, \hat{\eta}). \end{aligned} \quad (53)$$

On the other hand, since  $\mathcal{H}(\bar{\epsilon}, \hat{\eta}) \subset \mathcal{K}(\epsilon)$  we conclude from (41) that the upper bound  $\frac{1}{\|\phi(h)\|} < \frac{\eta(h)}{\|x\| - \epsilon}$  holds for every  $h \in \mathcal{H}(\bar{\epsilon}, \hat{\eta})$ . Putting together in (53), we have

$$\frac{\|\lambda(h)\|}{\eta(h)} < \frac{\eta(h)}{\|x\| - \epsilon} \frac{\epsilon}{\sqrt{\epsilon^2 - \bar{\epsilon}^2}} < \frac{\hat{\eta}}{\|x\| - \epsilon} \frac{\epsilon}{\sqrt{\epsilon^2 - \bar{\epsilon}^2}}.$$

Thus, from (48), we have

$$\hat{\sigma}(M(h)) \leq \frac{1}{\epsilon} (\|x\|^2 - \epsilon^2) \left( \frac{\|\lambda(h)\|}{\eta(h)} \right)^3 < \frac{\epsilon^2 (\|x\| + \epsilon)}{(\|x\| - \epsilon)^2} \left( \frac{\hat{\eta}}{\sqrt{\epsilon^2 - \bar{\epsilon}^2}} \right)^3. \quad (54)$$

**Uniform lower bound for  $\bar{\sigma}(M(h))$ .** We know that  $\sqrt{1 - \theta^2} < 1 - \frac{\theta^2}{2}$  for every  $\theta \in [0, 1]$ . Using this inequality in (48) for  $\bar{\sigma}(M(h))$  and simplifying, we see that

$$\bar{\sigma}(M(h)) \geq \frac{2\eta^3(h)}{(\|x\|^2 - \epsilon^2)} \geq \frac{2c^{*3}}{(\|x\|^2 - \epsilon^2)} \geq \frac{2\bar{\eta}^3}{(\|x\|^2 - \epsilon^2)}, \quad (55)$$

for every  $\bar{\eta} \in (0, c^*]$ . Collecting (54) and (55), we see that the minimum and maximum eigenvalues of the hessian are uniformly bounded over  $\mathcal{H}(\bar{\epsilon}, \hat{\eta})$ , and the bounds are

$$\begin{cases} \hat{\sigma}(\Delta^2 \eta(h)) < \frac{\epsilon^2 \hat{\eta}^3}{(\epsilon^2 - \bar{\epsilon}^2)^{3/2}} \frac{(\|x\| + \epsilon)}{(\|x\| - \epsilon)^2} \hat{\sigma}(\phi^a \circ \phi) & =: \beta(\bar{\epsilon}, \hat{\eta}), \\ \bar{\sigma}(\Delta^2 \eta(h)) \geq \frac{2\bar{\eta}^3}{(\|x\|^2 - \epsilon^2)} \bar{\sigma}(\phi^a \circ \phi) & =: \alpha(\bar{\eta}). \end{cases} \quad (56)$$

Finally,  $\eta : \mathcal{H}(\bar{\epsilon}, \hat{\eta}) \rightarrow [0, +\infty)$  is twice continuously differentiable with the maximum eigenvalue of the hessian being uniformly bounded above by  $\beta(\bar{\epsilon}, \hat{\eta})$ . It then follows that  $\eta : \mathcal{H}(\bar{\epsilon}, \hat{\eta}) \rightarrow [0, +\infty)$  is  $\beta(\bar{\epsilon}, \hat{\eta})$ -smooth and (12) holds. Moreover, if  $\phi$  is invertible in addition, then the minimum eigenvalue of the hessian is uniformly bounded below by  $\alpha > 0$ . Consequently, the mapping  $\eta : \mathcal{H}(\bar{\epsilon}, \hat{\eta}) \rightarrow [0, +\infty)$  is  $\alpha$ -strongly convex and the inequality (13) holds. The proof of the proposition is now complete.  $\square$

## 5.1. Proofs for reformulation as a smooth minimization problem

**Lemma 29** (Non-smooth reformulation). *Consider the LIP (1) under the setting of Assumption 2, then the LIP (1) is equivalent to the minimization problem*

$$\left\{ \min_{h \in B_c \cap \mathcal{K}(\epsilon)} \eta(h) \right\}. \quad (57)$$

In other words, the optimal value of (14) is equal to  $c^*$  and  $h^*$  is a solution to (14) if and only if  $c^* h^*$  is an optimal solution to (1).

*Lemma 29.* Recall that  $\Lambda = \{\lambda \in \mathbb{R}^n : \langle \lambda, x \rangle - \epsilon \|\lambda\| > 0\}$ ,  $B_c = \{h \in \mathbb{H} : c(\mathbb{H}) \leq 1\}$ , and  $L(\lambda, h) = 2\sqrt{\langle \lambda, x \rangle - \epsilon \|\lambda\|} - \langle \lambda, \phi(h) \rangle$ . The original LIP (1) was reformulated as the min-max problem. By considering  $r = 2, q = 0.5, \delta = 0$  in [22, Theorem 10] we see that the min-max problem

$$\left\{ \min_{h \in B_c} \sup_{\lambda \in \Lambda} L(\lambda, h) \right\}, \quad (58)$$

is equivalent to the LIP (1) with the optimal value of the min-max problem equal to  $c^*$ . Moreover, from [22, Theorem 10, assertion (ii)-a], it also follows that  $h^* \in \operatorname{argmin}_{h \in B_c} \left\{ \sup_{\lambda \in \Lambda} L(\lambda, h) \right\}$  if and only if  $c^*h^*$  is an optimal solution to the LIP (1). Solving for the maximization problem over  $\lambda$  in the min-max problem (58), in view of Proposition 21 we know that the maximum over  $\lambda$  is equal to  $\eta(h)$  whenever it is finite. Therefore, we get

$$h^* \in \operatorname{argmin}_{h \in B_c \cap \mathcal{K}(\epsilon)} \eta(h),$$

if and only if  $c^*h^*$  is an optimal solution to the LIP (1). The proof is now complete.  $\square$

*Theorem 5.* Under the setting of Assumption 2 we have  $B(x, \epsilon) \cap \operatorname{image}(\phi) \neq \emptyset$ . Thus, it follows from [22, Proposition 31-(ii)] and consequently, from [22, Theorem 10-(ii)-b], that the min-max problem

$$\left\{ \min_{h \in B_c} \sup_{\lambda \in \Lambda} 2\sqrt{\langle \lambda, x \rangle - \epsilon \|\lambda\|} - \langle \lambda, \phi(h) \rangle \right.$$

admits a saddle point solution. Moreover, every saddle point  $(h^*, \lambda^*) \in B_c \times \Lambda$  is such that  $h^* = (1/c^*)f^*$  where  $f^*$  is any optimal solution to the LIP (1), and  $\lambda^*$  is unique that satisfies

$$\lambda^* = \operatorname{argmax}_{\lambda \in \Lambda} 2\sqrt{\langle \lambda, x \rangle - \epsilon \|\lambda\|} - \langle \lambda, \phi(h^*) \rangle.$$

In view of Proposition 21-(ii), we conclude that  $h^* \in \operatorname{int}(\mathcal{K}(\epsilon))$ . Thus,  $e(f^*) = e(h^*) < \epsilon^2$ , this establishes assertion (i) of the lemma.

To prove the rest of the theorem, consider any  $\bar{\epsilon}, \hat{\eta} > 0$  such that  $e(f^*) \leq \bar{\epsilon}^2 < \epsilon^2$  and  $c^* \leq \hat{\eta}$ . Then for any  $h^* \in \operatorname{argmin}_{h \in B_c \cap \mathcal{K}(\epsilon)} \eta(h)$ , we conclude from Lemma 29 that  $c^*h^*$  is an optimal solution to the LIP (1). Consequently, assertion (i) of the proposition then implies that  $e(h^*) = e(c^*h^*) \leq \bar{\epsilon}^2$ . Thus, we have  $h^* \in \mathcal{K}(\bar{\epsilon})$ . Moreover, from Lemma 29 it is also immediate that  $\eta(h^*) = c^* \leq \hat{\eta}$ . Thus,  $h^* \in \mathcal{H}(\bar{\epsilon}, \hat{\eta})$ , and we have the inclusion

$$\operatorname{argmin}_{h \in B_c \cap \mathcal{K}(\epsilon)} \eta(h) \subset \mathcal{H}(\bar{\epsilon}, \hat{\eta}).$$

Since  $\mathcal{H}(\bar{\epsilon}, \hat{\eta}) \subset B_c \cap \mathcal{K}(\epsilon)$  to begin with, we conclude

$$\operatorname{argmin}_{h \in B_c \cap \mathcal{K}(\epsilon)} \eta(h) = \operatorname{argmin}_{h \in \mathcal{H}(\bar{\epsilon}, \hat{\eta})} \eta(h).$$

Now assertion (ii) of the theorem follows immediately as a consequence of Lemma 29.  $\square$

## 5.2. Proofs for reformulation as a strongly convex min-max problem

*Lemma 12.* Denoting  $\Lambda := \{\lambda \in \mathbb{R}^n : \langle \lambda, x \rangle - \epsilon \|\lambda\| > 0\}$  and  $\Lambda \ni \lambda \mapsto l(\lambda) = \sqrt{\langle \lambda, x \rangle - \epsilon \|\lambda\|}$ , it is known from [22] that the LIP (1) is equivalent to min-max problem

$$\left\{ \min_{h \in B_c} \sup_{\lambda \in \Lambda} L(\lambda, h) = 2l(\lambda) - \langle \lambda, \phi(h) \rangle. \right. \quad (59)$$

In particular, under the setting of Assumption 2, it follows that the min-max problem (59) admits a saddle point solution. It follows from [22, Theorem 10]) that a pair  $(h^*, \lambda^*)$  is a saddle point of (59) if and only if  $c^*h^*$  is an optimal solution to the LIP (1), and  $\lambda^* = \lambda(h^*)$  in view of Lemma 21.<sup>6</sup>

We prove the lemma by establishing that every saddle point solution to the min-max problem (59) is indeed a saddle point solution to the min-max problem (21) as well. We observe that the only difference between the min-max problems (21) and (59) is in their respective feasible sets  $\Lambda(\bar{\eta}, B)$  and  $\Lambda$  for the variable  $\lambda$ . Moreover, since  $\Lambda(\bar{\eta}, B) \subset \Lambda$ , it suffices to show that for every saddle point  $(h^*, \lambda^*)$  of (59), the inclusion  $\lambda^* \in \Lambda(\bar{\eta}, B)$  also holds. To establish this inclusion, we first recall from (39) that

$$l(\lambda^*) = l(\lambda(h^*)) = \eta(h^*) = c^* \geq \bar{\eta}.$$

Secondly, using (34) we also have

$$\begin{aligned} \|\lambda(h^*)\| &= \frac{\epsilon \eta(h^*)}{\|\phi(h^*)\| \sqrt{\epsilon^2 - e(h^*)}} \leq \frac{\epsilon \eta(h^*)}{\|\phi(h^*)\| \sqrt{\epsilon^2 - \bar{\epsilon}^2}} \quad \text{since } e(h^*) \in (\bar{\epsilon}^2, \epsilon^2), \\ &\leq \frac{\epsilon \eta^2(h^*)}{(\|x\| - \epsilon) \sqrt{\epsilon^2 - \bar{\epsilon}^2}} \quad \text{from (41),} \\ &\leq \frac{\epsilon \bar{\eta}^2}{(\|x\| - \epsilon) \sqrt{\epsilon^2 - \bar{\epsilon}^2}} = B. \end{aligned}$$

Thus,  $\lambda^* \in \Lambda(\bar{\eta}, B)$  and the lemma holds.  $\square$

**Lemma 30.** Consider  $x \in \mathbb{R}^n$  and  $\epsilon > 0$  such that  $\|x\| > \epsilon$ . Then the following assertions hold with regards to the mapping  $\Lambda \ni \lambda \mapsto l(\lambda) := \sqrt{\langle \lambda, x \rangle - \epsilon \|\lambda\|}$ .

- (i) the mapping  $\Lambda \ni \lambda \mapsto l(\lambda)$  is twice continuously differentiable and its hessian  $H(\lambda)$  evaluated at  $\lambda \in \Lambda$  is given by

$$H(\lambda) = \frac{-\epsilon}{2l(\lambda)\|\lambda\|} \left( \mathbb{I}_n - \frac{1}{\|\lambda\|^2} \lambda \lambda^\top \right) - \frac{1}{4(l(\lambda))^3} \left( x - \frac{\epsilon}{\|\lambda\|} \lambda \right) \left( x - \frac{\epsilon}{\|\lambda\|} \lambda \right)^\top. \quad (60)$$

- (ii) The smallest and largest absolute values of the eigenvalues of  $H(\lambda)$  denoted respectively by  $\bar{\sigma}(H(\lambda))$  and  $\hat{\sigma}(H(\lambda))$ , are given by

$$\begin{cases} \bar{\sigma} = \frac{(\|x\|^2 - \epsilon^2)}{8(l(\lambda))^3} \left( 1 - \sqrt{1 - \frac{8\epsilon(l(\lambda))^6}{(\|x\|^2 - \epsilon^2)^2 \|\lambda\|^3}} \right) \\ \hat{\sigma} = \frac{(\|x\|^2 - \epsilon^2)}{8(l(\lambda))^3} \left( 1 + \sqrt{1 - \frac{8\epsilon(l(\lambda))^6}{(\|x\|^2 - \epsilon^2)^2 \|\lambda\|^3}} \right). \end{cases} \quad (61)$$

*Lemma 30.* First of all, we observe that since  $\lambda \mapsto l(\lambda)$  is differentiable everywhere on  $\Lambda$ , and the gradients are given by  $\nabla l(\lambda) = \frac{1}{2l(\lambda)} \left( x - \frac{\epsilon}{\|\lambda\|} \lambda \right)$ . Differentiating again w.r.t.  $\lambda$ , we easily verify that the hessian is indeed as given by (60). First, suppose that  $\lambda$  and  $x$  are linearly independent, observe that the subspace  $S := \text{span}\{\lambda, x - \frac{\epsilon}{\|\lambda\|} \lambda\}$  is invariant under the linear transformation given by the hessian matrix  $H(\lambda)$ , and it is identity on the orthogonal complement of  $S$ . Then it is evident that the hessian has  $n - 2$  eigenvalues equal

<sup>6</sup>The inclusion  $\lambda^* \in c^* \Lambda$  provided in [22, (44), Theorem 10] turns out to be same as the condition  $\lambda^* = \lambda(h^*)$  under the setting of Assumption 2 for LIP (1). This can be formally established by observing from [22, Proposition 31] that  $\lambda^* = c^* \frac{x - c^* \phi(h^*)}{\|x - c^* \phi(h^*)\|_\phi}$ , and then, from [22, Lemma 33] we also have

$$\begin{aligned} \|x - c^* \phi(h^*)\|'_\phi &= \max_{h \in B_c} \langle x - c^* \phi(h^*), \phi(h) \rangle = \langle x - c^* \phi(h^*), \phi(h^*) \rangle \\ &= \|\phi(h^*)\| \sqrt{\epsilon^2 - e(h^*)}. \end{aligned}$$

to  $-\epsilon/l(\lambda)\|\lambda\|$  and the two other distinct eigenvalues corresponding to the restriction of  $H(\lambda)$  onto  $S$ . Selecting  $\{\lambda, x - \frac{\epsilon}{\|\lambda\|}\lambda\}$  as a basis for  $S$ , the linear mapping of the hessian is given by the matrix

$$T = \begin{pmatrix} 0 & \frac{\epsilon l(\lambda)}{2\|\lambda\|^3} \\ \frac{-1}{4l(\lambda)} & \frac{-(\|x\|^2 - \epsilon^2)}{4(l(\lambda))^3} \end{pmatrix}. \quad (62)$$

It is a straightforward exercise to verify that  $-\bar{\sigma}$  and  $-\hat{\sigma}$  are indeed the two distinct eigenvalues of  $T$  and consequently, the remaining two eigenvalues of the hessian  $H(\lambda)$ . Since the rest of the eigenvalues are  $-\epsilon/l(\lambda)\|\lambda\|$ , it remains to be shown that  $\bar{\sigma} \leq \epsilon/2l(\lambda)\|\lambda\| \leq \hat{\sigma}$ . We establish it by producing  $u_1, u_2 \in S$  such that

$$\bar{\sigma} \leq \frac{|\langle u_1, H(\lambda)u_1 \rangle|}{\|u_1\|^2} \leq \frac{\epsilon}{2l(\lambda)\|\lambda\|} \leq \frac{|\langle u_2, H(\lambda)u_2 \rangle|}{\|u_2\|^2} \leq \hat{\sigma}. \quad (63)$$

Observe that the inequalities  $\bar{\sigma} \leq \frac{|\langle u_1, H(\lambda)u_1 \rangle|}{\|u_1\|^2}$ , and  $\frac{|\langle u_2, H(\lambda)u_2 \rangle|}{\|u_2\|^2} \leq \hat{\sigma}$  readily hold for any  $u_1, u_2 \in S$  since  $-\bar{\sigma}, -\hat{\sigma}$  are the two eigenvalues of  $H(\lambda)$  when restricted to the subspace  $S$ . Considering  $u_1 = (l(\lambda))^2 x + \left(\|x\|^2 - \frac{\epsilon \langle \lambda, x \rangle}{\|\lambda\|}\right)\lambda$  and  $u_2 = \lambda - \frac{\|\lambda\|^2}{\langle \lambda, x \rangle}$ , it is easily verified that  $\langle x - \frac{\epsilon}{\|\lambda\|}\lambda, u_1 \rangle = 0$ , and  $\langle \lambda, u_2 \rangle = 0$ . Moreover, we also get the inequalities

$$\begin{cases} \langle u_1, H(\lambda)u_1 \rangle = \frac{-\epsilon}{2l(\lambda)\|\lambda\|} \|u_1\|^2 + \frac{\epsilon}{2l(\lambda)\|\lambda\|} \frac{|\langle \lambda, u_1 \rangle|^2}{\|\lambda\|^2} & \geq \frac{-\epsilon}{2l(\lambda)\|\lambda\|} \|u_1\|^2, \\ \langle u_2, H(\lambda)u_2 \rangle = \frac{-\epsilon}{2l(\lambda)\|\lambda\|} \|u_2\|^2 - \frac{1}{4(l(\lambda))^3} \left| \left\langle x - \frac{\epsilon}{\|\lambda\|}\lambda, u_2 \right\rangle \right|^2 & \leq \frac{-\epsilon}{2l(\lambda)\|\lambda\|} \|u_2\|^2. \end{cases}$$

Since the hessian  $H(\lambda)$  is negative semidefinite, the inequalities (63) are obtained at once.

To complete the proof for the case when  $\lambda$  and  $x$  are linearly dependent, we first see that the expressions in (61) are continuous w.r.t.  $\lambda$ . Also, it is evident that the mapping  $\Lambda \ni \lambda \mapsto H(\lambda)$  is continuous. Since the eigenvalues of a matrix vary continuously, these two limits must be the same. The proof is now complete.  $\square$

*Lemma 13.* We begin by first establishing that  $\bar{\sigma}(H(\lambda))$  and  $\hat{\sigma}(H(\lambda))$  as given in (30) satisfy the inequalities

$$\alpha' \leq 2\bar{\sigma}(H(\lambda)) \leq 2\hat{\sigma}(H(\lambda)) \leq \beta' \quad \text{for every } \lambda \in \Lambda(\bar{\eta}, B). \quad (64)$$

Since the mapping  $\Lambda \ni \lambda \mapsto H(\lambda)$  is concave, all the eigenvalues of the hessian  $H(\lambda)$  are non-positive (more importantly, real-valued). Thus,  $\frac{8\epsilon(l(\lambda))^6}{(\|x\|^2 - \epsilon^2)^2 \|\lambda\|^3} \leq 1$  since the square root term in (30) must be real valued.

To prove the lower bound for  $\bar{\sigma}(H(\lambda))$  in (64), we use the inequality that  $\sqrt{1 - \theta^2} < 1 - \frac{\theta^2}{2}$  for every  $\theta \in [0, 1]$ . Thereby,

$$\begin{aligned} \bar{\sigma}(H(\lambda)) &> \frac{(\|x\|^2 - \epsilon^2)}{8(l(\lambda))^3} \left( \frac{4\epsilon(l(\lambda))^6}{(\|x\|^2 - \epsilon^2)^2 \|\lambda\|^3} \right) \\ &= \frac{\epsilon}{2(\|x\|^2 - \epsilon^2)} \left( \frac{l(\lambda)}{\|\lambda\|} \right)^3 \geq \frac{\epsilon}{2(\|x\|^2 - \epsilon^2)} \left( \frac{\bar{\eta}}{B} \right)^3 \\ &= (1/2)\alpha' \quad \text{for all } \lambda \in \Lambda(\bar{\eta}, B). \end{aligned}$$

For  $\hat{\sigma}(H(\lambda))$ , using the inequality  $\sqrt{1 - \theta^2} < 1$  for  $\theta \in [0, 1]$ , we immediately get

$$\hat{\sigma}(H(\lambda)) \leq \frac{(\|x\|^2 - \epsilon^2)}{8(l(\lambda))^3} 2 \leq \frac{(\|x\|^2 - \epsilon^2)}{4\bar{\eta}^3} = (1/2)\beta' \quad \text{for all } \lambda \in \Lambda(\bar{\eta}, B).$$

Since  $\Lambda(\bar{\eta}, B) \subset \Lambda$ , for every  $\bar{\eta} \leq c^*$  and  $B > 0$ , it follows from assertion (i) of Lemma 30 that the mapping  $\Lambda(\bar{\eta}, B) \ni \lambda \mapsto -2l(\lambda)$  is also twice continuously differentiable. with the Hessian evaluated at  $\lambda$  being  $-2H(\lambda)$ . Moreover, the smallest and largest eigenvalues of this hessian are  $2\bar{\sigma}(H(\lambda))$  and  $2\hat{\sigma}(H(\lambda))$  respectively. In view of the inequalities (64), we see that the minimum eigenvalue of the hessian of the map  $\Lambda(\bar{\eta}, B) \ni \lambda \mapsto -2l(\lambda)$  is bounded below by  $\alpha'(\bar{\eta}, B)$  (and the maximum eigenvalue is bounded above by

$\beta'(\bar{\eta}))$ , uniformly over  $\lambda \in \Lambda(\bar{\eta}, B)$ . Thus, the mapping  $\Lambda(\bar{\eta}, B) \ni \lambda \mapsto -2l(\lambda)$  is  $\alpha'$ -strongly convex and  $\beta'$ -smooth. This completes the proof of the lemma.  $\square$

### 5.3. Proofs for step-size selection

**Lemma 31.** *Let  $\hat{\gamma}(h) := \max \{\gamma \in [0, 1] : h_\gamma \in \mathcal{K}(\bar{\epsilon})\}$ , then*

$$\hat{\gamma}(h) = \begin{cases} +\infty & a \geq 0, \\ \frac{-b - \sqrt{b^2 - 4ac}}{2a} & a < 0 \end{cases} \quad (65)$$

where  $a, b$  and  $c$  are defined in (66).<sup>7</sup>

*Proof of Lemma 31.* The maximum stepsize  $\hat{\gamma}(h)$  must satisfy  $h_\gamma \in \mathcal{K}(\bar{\epsilon})$ . Recall that  $h \in \mathcal{K}(\bar{\epsilon})$  if and only if  $\langle x, \phi(h) \rangle \geq \|\phi(h)\| \sqrt{(\|x\|^2 - \bar{\epsilon}^2)}$ . This gives rise to the following inequality  $\langle x, \phi(h_\gamma) \rangle \geq \|\phi(h_\gamma)\| \sqrt{(\|x\|^2 - \bar{\epsilon}^2)}$  which is of the form  $q(\gamma) \leq 0$  with

$$q(\gamma) = a\gamma^2 + b\gamma + c, \quad (67)$$

with the definitions for  $a, b$  and  $c$  as described in proposition 31. Three different domains for  $a$  are considered separately

- (1)  $a > 0$ . Since  $c \geq 0$ , we have that  $\frac{a}{c} > 0$ . Note that the domain must be continuous since  $\eta(h)$  is a convex function and therefore  $q(\gamma) \leq 0$ . This results in the domain  $\gamma \in [0, +\infty]$ .
- (2)  $a = 0$ . Since  $c \geq 0$  we have  $|\langle x, \phi(h) \rangle| \geq \sqrt{\|x\|^2 - \bar{\epsilon}^2} \|\phi(h)\|$ . While  $a = 0$ , we have  $|\langle x, \phi(d) \rangle| = \sqrt{\|x\|^2 - \bar{\epsilon}^2} \|\phi(d)\|$ . Combining these two equations and applying Cauchy-Schwartz we get  $|\langle x, \phi(h) \rangle| \|\langle x, \phi(d) \rangle| \geq (\|x\|^2 - \bar{\epsilon}^2) \langle \phi(d), \phi(h) \rangle$ . From this equation it is obvious that we have  $b \geq 0$  and therefore  $\gamma = \frac{-c}{2b} < 0$ . This gives the following domain  $\gamma \in [0, +\infty]$ .
- (3)  $a < 0$ . Since  $c \geq 0$ , the product of the roots of quadratic equation  $q(\gamma) = 0$  are real and of opposite signs. Therefore,  $\hat{\gamma}(h)$  can be picked as the positive root of the quadratic equation  $q(\gamma) = 0$ , given by  $\gamma \in [0, \frac{-b - \sqrt{b^2 - 4ac}}{2a}]$ .

$\square$

*Proposition 18.* In terms of  $\hat{\gamma}(h)$ , the line search problem (29) reduces to

$$\gamma(h) = \begin{cases} \operatorname{argmin} & \eta(h + \gamma d(h)). \\ \gamma \in [0, \hat{\gamma}(h)] & \end{cases} \quad (68)$$

The explicit solution to (68) is easily described since it is a scalar problem over an interval.

Since  $h \mapsto \eta(h)$  is convex, the mapping  $[0, \hat{\gamma}(h)] \ni \gamma \mapsto \eta(h_\gamma)$  is also convex. Clearly, if  $\frac{\partial \eta(h_\gamma)}{\partial \gamma}|_{\gamma=0} \geq 0$ , it follows from convexity that  $\gamma(h) = 0$ . Along similar analogy, if  $\frac{\partial \eta(h_\gamma)}{\partial \gamma}|_{\gamma=\hat{\gamma}(h)} \leq 0$ , then  $\gamma(h) = \hat{\gamma}(h)$ . Finally, if  $\frac{\partial \eta(h_\gamma)}{\partial \gamma}|_{\gamma=0} < 0 < \frac{\partial \eta(h_\gamma)}{\partial \gamma}|_{\gamma=\hat{\gamma}(h)}$ , then from intermediate value theorem, there must exist some  $\gamma(h) \in (0, \hat{\gamma}(h))$  such that  $0 = \frac{\partial \eta(h_\gamma)}{\partial \gamma}|_{\gamma=\gamma(h)}$ . This reduces to the quadratic equation  $r\gamma^2 + s\gamma + u = 0$  for values of  $r, s, u$  specified in (31), whose solutions are  $\gamma = \frac{-s \pm \sqrt{s^2 - 4ru}}{2r}$ . It is guaranteed that one of these roots is positive and lies in the interval  $(0, \hat{\gamma}(h))$ , which is selected as  $\gamma(h)$ .  $\square$

$$\begin{aligned} a &= \|\phi(d)\|^2 (\bar{\epsilon}^2 - e(d)) \\ b &= 2 \langle x, \phi(h) \rangle \langle x, \phi(d) \rangle - (\|x\|^2 - \bar{\epsilon}^2) \langle \phi(h), \phi(d) \rangle \\ c &= \|\phi(h)\|^2 (\bar{\epsilon}^2 - e(h)). \end{aligned} \quad (66)$$

## 6. APPENDIX

## 6.1. Tuning methods

**Tuning CP.** The CP algorithm in [10], contains three tuning parameters; the primal step size  $\sigma$ , the dual step size  $\tau$ , and the momentum parameter  $\theta$ . Both  $\sigma$  and  $\tau$  are set to  $\sigma = \frac{1}{\sigma_m}$  and  $\tau = \frac{1}{\sigma_m}$  with  $\sigma_m$  representing the maximum singular value of the linear mapping  $\phi$  [10]. The value of the momentum step parameter  $\theta \in [0, 1]$  is hand-tuned.

Figure 10 shows the image denoising results of the tuning experiment for  $\theta$ . The first metric used in this graph is the average distance to optimality  $\|f - f^*\|$  of all patches, where  $f^*$  is the optimal solution. The second metric is the total cost of the objective function of Problem (4) of all patches at each iteration. In the top graph of Figure 10, it can be seen that the differences between the different values of  $\theta$  are negligible. In the bottom graph, observe that  $\theta = 0.5$  results in a small undershoot and  $\theta = 0.7$  and  $\theta = 0.8$  show slower convergence compared to  $\theta = 0.6$ . Therefore,  $\theta = 0.6$  was chosen. This parameter is kept constant throughout all experiments since other patch size experiments gave similar results.

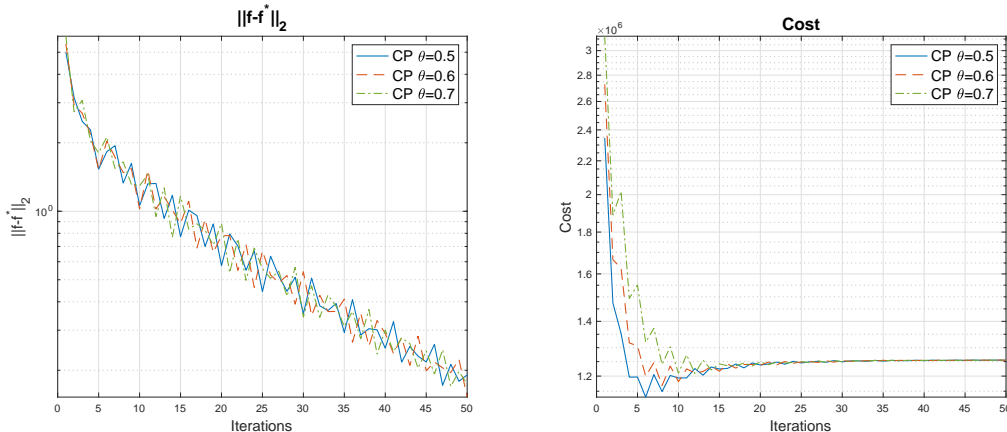


FIGURE 10. CP image denoising results for  $\theta = \{0.5, 0.6, 0.7\}$  for the  $200 \times 200$  ‘cameraman’ image with sliding patch approach for the patch size  $32 \times 32$ ,  $\sigma = 0.0055$ ,  $\epsilon = \sqrt{\sigma n}$  for 50 iterations.

**Tuning C-SALSA.** C-SALSA has one tuning parameter; the augmented Lagrangian penalty parameter  $\mu$  [1]. For patch sizes smaller than  $64 \times 64$ , we take  $\mu = 2.5$ , and for patch sizes bigger than or equal to  $64 \times 64$ , we take  $\mu = 3$ . In Figure 11, the different graphs show the different results for  $\mu = \{2, 2.5, 3\}$  for an experiment with  $32 \times 32$  patches. It can be seen that the higher  $\mu$  is chosen, the faster convergence in the distance to optimality graph. However, it also results in higher cost for the initial iterations, shown in the second graph. Therefore, a trade-off was made, and the value  $\mu = 2.5$  was chosen. The same experiment was done for the  $64 \times 64$  patches which resulted in  $\mu = 3$ .

**Tuning FLIPS.** Applying FLIPS with the Quadratic Oracle of Algorithm 1 contains two tuning parameters; the acceleration parameter  $\rho$ , and the smoothness parameter  $\beta$ . The Quadratic Oracle was applied throughout the experiments since it outperforms the Linear Oracle in terms of speed for the denoising problem. The Linear Oracle does not require any tuning parameter.

Since many vectors and matrices in this algorithm contain just a few non-zeros, the MATLAB function `sparse` is used throughout the algorithm to reduce storage. This function only stores the non-zero values

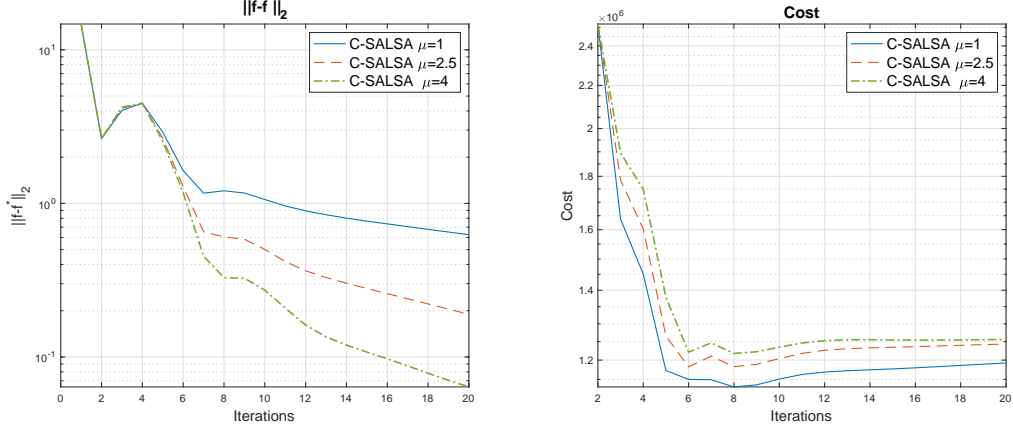


FIGURE 11. C-SALSA image denoising results for  $\mu = \{2, 2.5, 3\}$  for the  $200 \times 200$  ‘cameraman’ image with sliding patch approach for the patch size  $32 \times 32$ ,  $\sigma = 0.0055$ ,  $\epsilon = \sqrt{\sigma n}$  for 50 iterations.

and their positions and assumes all others to be zero. Applying this function did not significantly improve the speed for the other methods.

Ten different values for  $\beta^{-1}$  and  $\rho$  are performed in a grid search method. The number of iterations needed until the sub-optimality  $\eta - \eta^*$  converges to 1% of its original value is shown on the left in Figure 12. On the right of Figure 12, the sub-optimality is shown for three different values for  $\beta^{-1}$  with  $\rho = 0.7$  fixed. The value  $\rho = 0.7$  is chosen throughout the experiments since it appears to be less sensitive to changes in  $\beta^{-1}$  than higher values.

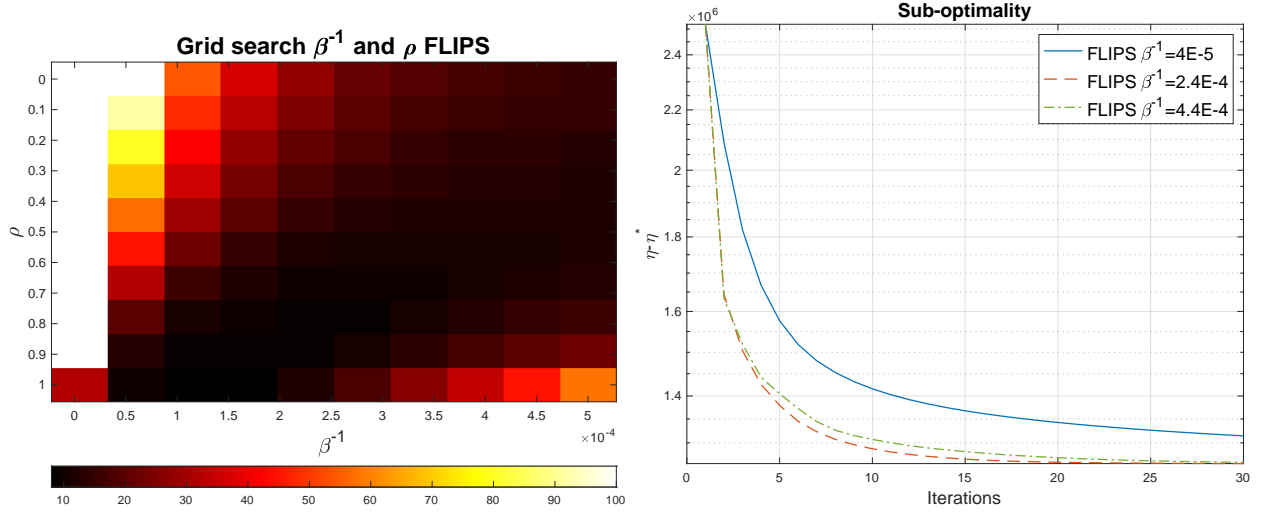


FIGURE 12. Left: Number of iterations until convergence to 1% of  $\eta - \eta^*$  compared to the first iteration for a grid search with  $\rho = [0, 1]$  and  $\beta^{-1} = [5 \cdot 10^{-6}, 5 \cdot 10^{-4}]$ . Right: FLIPS image denoising results for  $\beta^{-1} = \{4 \cdot 10^{-5}, 2.4 \cdot 10^{-4}, 4.4 \cdot 10^{-4}\}$  for the  $200 \times 200$  ‘cameraman’ image with sliding patch approach for the patch size  $32 \times 32$ ,  $\rho = 0.7$ ,  $\sigma = 0.0055$ ,  $\epsilon = \sqrt{\sigma n}$  for 50 iterations.



## REFERENCES

- [1] M. V. AFONSO, J. M. BIOUCAS-DIAS, AND M. A. T. FIGUEIREDO, *An Augmented Lagrangian Approach to the Constrained Optimization Formulation of Imaging Inverse Problems*, IEEE Transactions On Image Processing, (2009).
- [2] M. AHARON, M. ELAD, AND A. BRUCKSTEIN, *K-SVD: An algorithm for designing overcomplete dictionaries for sparse representation*, IEEE Transactions on Signal Processing, 54 (2006), pp. 4311–4322.
- [3] A. BECK AND M. TEBoulLE, *A fast iterative shrinkage-thresholding algorithm for linear inverse problems*, SIAM Journal on Imaging Sciences, 2 (2009), pp. 183–202.
- [4] D. P. BERTSEKAS, *Control of uncertain systems with a set-membership description of the uncertainty.*, PhD thesis, Massachusetts Institute of Technology, 1971.
- [5] S. BOYD, L. XIAO, AND A. MUTAPCIC, *Subgradient methods*, Notes for EE392o, (2003).
- [6] E. J. CANDÈS AND T. TAO, *Near-optimal signal recovery from random projections: Universal encoding strategies?*, IEEE transactions on information theory, 52 (2006), pp. 5406–5425.
- [7] E. J. CANDÈS AND M. B. WAKIN, *An introduction to compressive sampling [a sensing/sampling paradigm that goes against the common knowledge in data acquisition]*, IEEE signal processing magazine, 25 (2008), pp. 21–30.
- [8] E. J. CANDÈS AND B. RECHT, *Exact matrix completion via convex optimization*, Foundations of Computational Mathematics, 9 (2009), pp. 717–772.
- [9] A. CHAMBOLE AND T. POCK, *A first-order primal-dual algorithm for convex problems with applications to imaging*, tech. rep., HAL open science, 2010.
- [10] ———, *On the ergodic convergence rates of a first-order primal-dual algorithm*, Mathematical Programming, 159 (2016), pp. 253–287.
- [11] D. L. DONOHO, *Compressed sensing*, IEEE Transactions on Information Theory, 52 (2006), pp. 1289–1306.
- [12] D. L. DONOHO, *For Most Large Underdetermined Systems of Linear Equations the Minimal 1-norm Solution Is Also the Sparsest Solution*, Communications on Pure and Applied Mathematics, 59 (2006), pp. 797–829.
- [13] J. DUCHI, S. SHALEV-SCHWARTZ, Y. SINGER, AND T. CHANDRA, *Efficient Projections onto the  $l_1$ -Ball for Learning in High Dimensions*, tech. rep., Proceedings of the 25th International Conference on Machine Learning, 2008.
- [14] M. ELAD AND M. AHARON, *Image denoising via sparse and redundant representations over learned dictionaries*, IEEE Transactions on Image processing, 15 (2006), pp. 3736–3745.
- [15] M. FRANK AND P. WOLFE, *An algorithm for quadratic programming*, Naval Research Logistics, (1956).
- [16] S. GLEICHMAN AND Y. C. ELДАР, *Blind Compressed Sensing*, IEEE Transactions on Information Theory, 57 (2011), pp. 6958–6975.
- [17] M. JAGGI, *Revisiting Frank-Wolfe: Projection-Free Sparse Convex Optimization*, tech. rep., Ecole Polytechnique, 2013.
- [18] M. NAGAHARA, D. E. QUEVEDO, AND D. NEŠIĆ, *Maximum hands-off control: a paradigm of control effort minimization*, IEEE Transactions on Automatic Control, 61 (2015), pp. 735–747.
- [19] B. A. OLSHAUSEN AND D. J. FIELDT, *Sparse Coding with an Overcomplete Basis Set: A Strategy Employed by V1 ?*, Tech. Rep. 23, 1997.
- [20] B. RECHT, M. FAZEL, AND P. PARRILO, *Guaranteed minimum-rank solutions of linear matrix equations via nuclear norm minimization*, SIAM review, 52 (2010), pp. 471–501.
- [21] F. REDEL, *Flips*. <https://github.com/FFRedel/FLIPS.git>, 2022.
- [22] M. R. SHERIFF AND D. CHATTERJEE, *Novel min-max reformulations of Linear Inverse Problems*, arXiv preprint arXiv:2007.02448., (2020).
- [23] M. YAGHOUBI AND M. E. DAVIES, *Compressible dictionary learning for fast sparse approximations*, in IEEE Workshop on Statistical Signal Processing Proceedings, 2009, pp. 662–665.
- [24] W. H. YANG, *On generalized holder inequality*, 1991.
- [25] YE. E. NESTEROV, *A method of solving a convex programming problem with convergence rate  $O(1/k^2)$* , Soviet Math dokl., 27 (1983).